Author Manuscript

Author Manuscript

Author Manuscript

Author Manuscript

HHS Public Access

Author manuscript

Cell Rep. Author manuscript; available in PMC 2019 January 03.

Published in final edited form as:

Cell Rep. 2018 November 27; 25(9): 2510–2523.e4. doi:10.1016/j.celrep.2018.10.106.

Six3 and Six6 Are Jointly Required for the Maintenance of Multipotent Retinal Progenitors through Both Positive and Negative Regulation

Diacou Raven[1], **Zhao Yilin**[1], **Zheng Deyou**[1], **Cvekl Ales**[1], and **Liu Wei**[1,2,*]

[1]Departments of Ophthalmology and Visual Sciences and Genetics, Albert Einstein College of Medicine, New York, NY 10461, USA

[2]Lead Contact

SUMMARY

Gene regulation of multipotent neuroretinal progenitors is partially understood. Through characterizing *Six3* and *Six6* double knockout retinas (DKOs), we demonstrate Six3 and Six6 are jointly required for the maintenance of multipotent neuroretinal progenitors. Phenotypes in DKOs were not found in either *Six3* nulls or *Six6* nulls. At the far periphery, ciliary margin (CM) markers Otx1 and Cdon together with Wnt3a and Fzd1 were ectopically upregulated, whereas neuroretinal progenitor markers Sox2, Notch1, and Otx2 were absent or reduced. At the mid periphery, multi-lineage differentiation was defective. The gene set jointly regulated by Six3 and Six6 significantly overlapped with the gene networks regulated by WNT3A, CTNNB1, POU4F2, or SOX2. Stimulation of Wnt/β-catenin signaling by either Wnt-3a or a GS3Kβ inhibitor promoted CM progenitors at the cost of neuroretinal identity at the periphery of eyecups. Therefore, Six3 and Six6 together directly or indirectly suppress Wnt/β-catenin signaling but promote retinogenic factors for the maintenance of multipotent neuroretinal progenitors.

In Brief

Gene regulation of multipotent retinal progenitor cells is partially understood. Through genetic, molecular, and transcriptomic characterization of *Six3* and *Six6* compound null retinas in mice, Diacou et al. demonstrate that Six3 and Six6 jointly suppress Wnt/β-catenin signaling but promote the expression of retinogenic factors to maintain multipotent retinal progenitor cells.

Graphical Abstract

This is an open access article under the CC BY-NC-ND license (http://creativecommons.org/licenses/by-nc-nd/4.0/).

*Correspondence: wei.liu@einstein.yu.edu.

AUTHOR CONTRIBUTIONS

R.D. performed and analyzed experiments; Y.Z. analyzed RNA-seq data under the supervision of D.Z.; A.C. edited the manuscript; and W.L. designed, performed, and analyzed experiments and wrote the manuscript. All authors read and approved the manuscript.

DECLARATION OF INTERESTS

The authors declare no competing interests.

SUPPLEMENTAL INFORMATION

Supplemental Information includes seven figures and four tables and can be found with this article online at https://doi.org/10.1016/j.celrep.2018.10.106.

Author Manuscript Author Manuscript Author Manuscript Author Manuscript

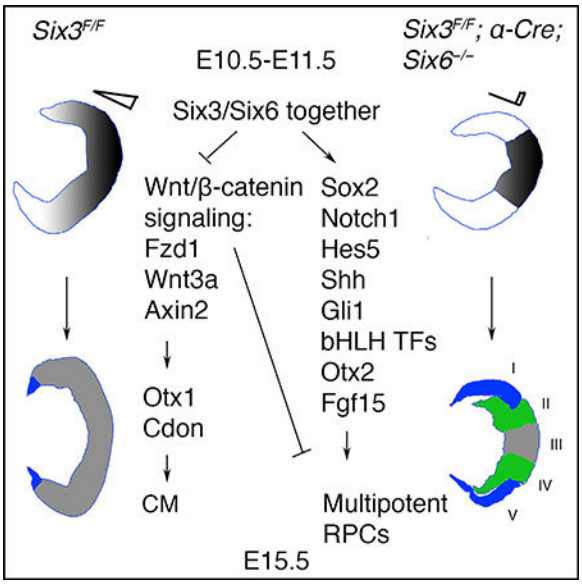

INTRODUCTION

Cell fate specification and maintenance are fundamental for tissue formation in embryogenesis. In murine retinal development, specified early retinal progenitors are marked by the expression of eye field transcription factors, including Six3, Pax6, Rax, Otx2, and Lhx2 in embryonic day 8.0 (E8.0)–8.5 embryos (Liu et al., 2010). From the early retinal progenitors, neuroretinal (NR) progenitors and retinal pigment epithelial (RPE) progenitors, marked by the expression of Vsx2 and Mitf, respectively, are then specified and partitioned into the inner and outer layers of optic cups by E10.5 (Horsford et al., 2005; Liu et al., 2010). At the periphery of the NR abutting RPE in optic cups, ciliary margin (CM) progenitors are specified at E12.5, as indicated by the expression of Otx1 and Cdon (Bélanger et al., 2017; Liu et al., 2007). CM tissue is also found at the transition zone between fibroblast growth factor (FGF)-induced RPE-derived NR tissue and the endogenous RPE in chicks (Dias da Silva et al., 2007). Activation of Wnt/β-catenin signaling is necessary and sufficient for CM specification in chicks and mice (Cho and Cepko, 2006; Esteve et al., 2011; Fotaki et al., 2013; Heavner et al., 2014; Kinoshita et al., 2016; Kubo et al., 2003; Liu et al., 2007). CM progenitors give rise to both retinal neurons and non-pigmented ciliary epithelial cells in mice (Bélanger et al., 2017; Marcucci et al., 2016). Despite the advances, it is unclear how NR maintenance and CM specification are coordinated resulting in a tapered CM zone in the peripheral NR.

NR progenitors in optic cups are multipotent, generating retinal neurons and Müller glia in an evolutionary conserved order through coordinated retinal cell differentiation and maintenance of a pool of NR progenitors (Cepko, 2014). Transcription factor Pax6 is required for the multipotency of NR progenitors through direct transcriptional activation of retinogenic bHLH factors (Marquardt et al., 2001). Notably, *Pax6* inactivation in peripheral optic cups reveals divergent progenitor pools of NR progenitors, since Pax6 prevents premature activation of a photoreceptor-differentiation pathway at the periphery but

Author Manuscript Author Manuscript Author Manuscript Author Manuscript

regulates the multipotency of NR progenitors in more central regions (Oron-Karni et al., 2008). Intrinsic differences in NR progenitors are also demonstrated by recent fate mapping and live imaging studies (Cepko, 2014). Besides Pax6, Hh signaling regulator Sufu is required to maintain the multipotency and identity of NR progenitors through antagonizing Hh/Gli2 signaling (Cwinn et al., 2011); transcription factor Sox2 is required for NR progenitor competence and NR-CM boundary in a dose-dependent manner (Heavner et al., 2014; Matsushima et al., 2011; Taranova et al., 2006). Despite these findings, it is unclear how regulatory genes for the multipotency of NR progenitors are involved in CM specification.

We have demonstrated that homeodomain transcription factor Six3 is an essential cell-fate determinant in NR specification. In mice, starting at E7.5–8.0, Six3 is expressed at the anterior neural plate, eye field, optic vesicles, and optic cups (Lagutin et al., 2003; Liu et al., 2010). Germline *Six3 inactivation* ablates both rostral forebrain and eye field following a rostral expansion of Wnt1 (Lagutin et al., 2003). Conditional *Six3* inactivation using Rx-Cre ablates NR specification but expands RPE following a rostral expansion of Wnt8b (Liu et al., 2010). Six3 in a small population of progenitors at E8.5 is required for NR specification through suppressing Wnt8b, maintaining FGF/ERK signaling, and cell survival (Liu and Cvekl, 2017). Six6, a paralog of Six3, is expressed in optic vesicles starting at E8.5–9.0, a later stage compared to Six3, and is largely co-localized with Six3 in the progenitors in optic vesicles and optic cups (Jean et al., 1999; Liu and Cvekl, 2017). Neither *Six3* inactivation at E9.5–10.5 nor *Six6* deletion (Li et al., 2002) overtly affect NR specification, but *Six3* inactivation at E9.5 together with *Six6* deletion ablates NR specification, indicating genetic interactions between *Six3* and *Six6* in retinal development (Liu and Cvekl, 2017).

To test the hypothesis that Six3 and Six6 together play a role in specified NR progenitors, here we conditionally inactivated *Six3* using *α-Cre* at E10.5 (Marquardt et al., 2001) together with *Six6* deletion (DKO; *Six3* and *Six6* double knockout). Phenotypes in the DKO retinas were not found in either *Six3* null or *Six6* null retinas: the CM was expanded at the cost of NR progenitors at the far periphery, whereas multi-lineage differentiation was defective at the mid periphery. Through phenotypic analysis of DKO retinas, RNA sequencing (RNA-seq) transcriptome profiling, Ingenuity Pathway Analysis, and stimulation of Wnt/β-catenin signaling in mouse eyecup cultures, we conclude that Six3 and Six6 jointly suppress Wnt/β-catenin signaling but promote retinogenic factors to maintain multipotent NR progenitors in mice.

RESULTS

Six3 Exhibits in a Gradient in E10.5–E11.5 Neuroretina, and *Six3* and *Six6* Compound Deletion (DKO) Causes Morphological Abnormalities

To determine Six3 and Six6 functions after NR specification, we conditionally inactivated *Six3* at E10.5 using *α-Cre* (Marquardt et al., 2001) in combination with *Six6* deletion (Li et al., 2002). In E10.5 mouse retina, Six3 protein expression exhibited a gradient along the peripheral-central axis with high levels in central regions (Figure 1A), consistent with a *Six3* mRNA gradient in E12.5 retina described previously (Martinez-Morales et al., 2001). Similarly, *Six6* mRNA expression also displayed a peripheral-central gradient in E10.5

Author Manuscript Author Manuscript Author Manuscript Author Manuscript

retina (Liu and Cvekl, 2017). In contrast, Pax6 protein expression formed an inverse gradient (Figures 1A and 1B). The graded Six3 expression persisted at E11.5 (Figure 1D). Although R26R reporter expression for *α-Cre* was detected as early as E10.5 (Figure 1C), Six3 protein deletion in $Six3^{F/F}$;*α-Cre* retinas was detected as early as E11.5 (Figures 1D and 1E). Consistent with our previous findings that all retinal cell types are present in postnatal *Six3* mutant retinas in which Six3 is deleted starting at E9.5 (Liu and Cvekl, 2017), *Six3* deletion at E10.5 did not overtly affect the expression of major NR progenitor markers in E14.5 $Six3^{F/F}$;*α-Cre* retinas (Figure S1). Similarly, *Six6* deletion did not affect retinal cell fate determination (Li et al., 2002), which was confirmed in our studies (data not shown). In contrast, inactivation of both *Six3* and *Six6* ($Six3^{F/F}$;*α-Cre*;$Six6^{-/-}$, referred to as DKO hereafter) caused major retinal abnormalities not seen in either conditional *Six3* nulls or *Six6* nulls (Figures 1F–1W). In E14.5 control retinas, newly differentiated retinal neurons formed a distinguishable layer (dotted line in Figure 1F). A similar retinal structure was found in both $Six3^{F/F}$;$Six6^{-/-}$ retinas and $Six3^{F/F}$;*α-Cre*;$Six6^{+/-}$ retinas (Figures 1G and 1H). In E14.5 DKO retinas, however, the layer of newly differentiated retinal neurons was absent in peripheral regions but remained in central regions (Figure 1I). In addition, an abrupt change in retinal thickness was found within the peripheral retina, resulting in far-peripheral and mid-peripheral regions (arrowhead in Figure 1I; see also Figure 1O for R26R reporter expression for *α-Cre*, Figures 2D, 3D, and 4D for efficient Six3 deletion in both far- and mid-peripheral regions, and Figures 4H, 4P, and 4X for distinct gene expression profiles in far- and mid-peripheral regions). Interestingly, GFP expression (Cre-IRES-GFP) was expanded centrally in E14.5 DKO retinas compared to that in conditional *Six3* null retinas (Figures 1J and 1K). On postnatal day 11, the control, conditional *Six3* null (Figures 1L and 1M), and *Six6* null retinas (data not shown) were translucent, but DKO retinas were opaque except for in a narrow central band in which R26R reporter expression for *α-Cre* was absent (Figures 1N and 1O). In addition, DKO retinas displayed severe degenerations at far-peripheral regions (arrow-heads in Figure 1N). On sections, DKO retinas lacked a laminar structure and comprised sparsely dispersed cells (Figures 1P–1W; see also Figures 5, S6, and S7 for molecular characterization). Collectively, *Six3* deletion at E10.5 using *α-Cre* together with *Six6* deletion drastically disrupts retinal cell differentiation.

NR Progenitors Are Defective, and Retinal Cell Differentiation Is Affected in E14.5 DKO Retinas

We sought to determine the molecular mechanisms underlying the phenotypes in DKO retinas. In E14.5 DKO retinas, Six3 was efficiently deleted except for in a narrow central region where *α-Cre* was inactive (Figures 2A–2D). Sox2, a dose-dependent essential regulator of NR progenitor competence and NR-CM boundary, regulates Notch1 expression in the NR (Heavner et al., 2014; Matsushima et al., 2011; Taranova et al., 2006). Sox2 expression was normal in both *Six6* null retinas and $Six3^{F/F}$;*α-Cre* retinas but was significantly reduced in the peripheral regions of DKO retinas (Figures 2E–2H). Accordingly, Notch1 was nearly absent (Figures 2I–2L), and Hes5 was severely reduced (Figures S2A–S2D) in DKO retinas. Gli1, a target of Shh signaling (Lee et al., 1997), is expressed in NR progenitors but not in the CM. Gli1 is increased in *Sufu* null retinas in which multipotency of NR progenitors is disrupted (Cwinn et al., 2011). In DKO retinas, Gli1 expression was absent in far-peripheral regions and severely reduced in mid-peripheral

Author Manuscript Author Manuscript Author Manuscript Author Manuscript

regions compared to the control retinas (Figures 2M–2P), indicating phenotype differences between DKO retinas and *Sufu* null retinas. Ascl1, a bHLH transcription factor that defines a competence-restricted lineage and is required for cell proliferation (Brzezinski et al., 2011; Marquardt et al., 2001), is expressed in NR progenitors but not in the CM. In DKO retinas, Ascl1 was absent in far-peripheral regions and severely reduced in mid-peripheral regions compared to the control retinas (Figures 2Q–2T). Neurod4 and Neurod1 are jointly required for amacrine cell differentiation, and misexpression of these bHLH genes alone induces rod genesis (Inoue et al., 2002). In DKO retinas, Neurod4 expression was severely reduced in far-peripheral regions and reduced in mid-peripheral regions (Figures S2E–S2H). Fzd5, a receptor of Wnt signaling proteins, is expressed in the NR; *Fzd5* inactivation in germline disrupts optic cup formation (Burns et al., 2008). In DKO retinas, Fzd5 was severely reduced in far-peripheral regions and moderately reduced in mid-peripheral regions (Figures S2I–S2L). Cyclin kinase inhibitor p57 is elevated in *Six6* null retinas (Li et al., 2002). In the control retinas, p57 was moderately expressed in the CM but barely expressed in the NR (Figure S2M). In $Six3^{F/+}$;*α-Cre*;$Six6^{-/-}$ retinas, p57 expression was marginally increased (Figures S2M and S2O). In DKO retinas, p57 expression was ectopically upregulated in far-peripheral regions (Figures S2M and S2P), indicating a CM expansion. Atoh7, a bHLH transcription factor required for retinal ganglion cell differentiation (Brown et al., 1998; Wang et al., 2001), was severely reduced in the peripheral regions of DKO retinas (Figures S3A–S3D). Banded Atoh7 expression in peripheral DKO retinas could be caused by incomplete *Six3* deletion and/or represent Atoh7 expression in amacrine cell lineages (Feng et al., 2010), since amacrine cell differentiation was largely unaffected in DKO retinas (see also Figures 4P, 5I, 5L, S5L, S6D, S6H, S6L, and S6P). Neurog2, a NR progenitor marker (Marquardt et al., 2001), was reduced in far-peripheral regions of DKO retinas (Figures S3E–S3H). Fgf15, a marker for NR progenitors (Burns et al., 2008), was also reduced in far-peripheral regions of DKO retinas (Figures S3I–S3L). The reduction in Fgf15 expression explained the posterior expansion of lens epithelium in DKOs (Figures 1I and S2P), since retina-derived FGFs promote lens fiber differentiation (Lovicu and McAvoy, 2005). Collectively, NR progenitors are grossly normal in conditional *Six3* null or *Six6* null retinas but are strikingly defective in DKO retinas.

To evaluate early retinal differentiation, we examined retinal neurons in E14.5 DKO retinas. Six3 was efficiently deleted in $Six3^{F/F}$;*α-Cre*;$Six6^{+/-}$ retinas and DKO retinas (Figures 3C and 3D). Pou4f2 (also known as Brn3b), a POU domain transcription factor required for retinal ganglion cell development (Gan et al., 1996), was grossly normal in both $Six3^{F/F}$;$Six6^{-/-}$ and $Six3^{F/F}$; *α-Cre*;$Six6^{+/-}$ retinas (Figures 3A–3G). In DKO retinas, however, Pou4f2 was nearly absent in far-peripheral regions and severely reduced and disorganized in mid-peripheral regions (Figure 3H), indicating defective retinal ganglion cell differentiation. Tubb3 and p27 are expressed in early born retinal neurons, including retinal ganglion cells. In DKO retinas, Tubb3 and p27 were severely reduced in far-peripheral regions (Figures 3L and 3P), confirming the defects in early retinal differentiation. Pax6, a transcription factor essential for the multipotency of NR progenitors (Marquardt et al., 2001), was expressed in NR progenitors, CM progenitors (bracket in Figure 3Q), and early-differentiated retinal neurons in the control retinas (Figure 3Q). In DKO retinas, Pax6 expression remained and was even upregulated in far-peripheral regions (bracket in Figures

Author Manuscript Author Manuscript Author Manuscript Author Manuscript

3Q and 3T), indicating that NR defects in DKO retinas were not caused by Pax6 down-regulation. Collectively, early retinal cell differentiation is largely normal in both *Six3*$^{F/F}$;*Six6*$^{-/-}$ and *Six3*$^{F/F}$;*α-Cre*;*Six6*$^{+/-}$ retinas but is remarkably defective in DKO retinas.

To assess cell proliferation in DKO retinas, we examined Ccnd1 (also known as cyclin D1) and pH3. Ccnd1 was highly expressed in the NR but marginally expressed in the CM in the control retinas (Figure S4A). Similar Ccnd1 expression was found in both *Six3*$^{F/F}$;*Six6*$^{-/-}$ retinas and *Six3*$^{F/F}$;*α-Cre*;*Six6*$^{+/-}$ retinas (Figures S4A–S4C). In DKO retinas, Ccnd1 was nearly absent in peripheral NR (Figures S4A and S4D), indicating severe defects in cell proliferation. In the control retinas, pH3 positive cells were found at the apical surface of the NR (Figure S4E). In DKO retinas, pH3 positive cells were reduced in density in far-peripheral regions (Figures S4E–S4H and S4M) and occasionally mis-localized in mid-peripheral regions (Figure S4H) likely due to the defects in apical junctions (Figures S4O and S4R). Meanwhile, apoptosis was increased in peripheral DKO retinas (Figures S4I–S4L and S4N), likely caused by altered or mixed cell identity.

Taken together, although either conditional Six3 null or Six6 null retinas are grossly normal, DKO retinas display striking defects in NR identity and differentiation.

Loss of NR Identity in DKO Retinas Is Accompanied by Ectopic Upregulation of Wnt/β-Catenin Signaling and CM Markers

We sought to determine whether the defects in NR identity and differentiation in DKO retinas were correlated to cell fate changes. At E15.5, Six3 was efficiently deleted at the peripheral regions in both *Six3*$^{F/F}$;*α-Cre* retinas and DKO retinas (Figures 4A–4D). Six3 was unaffected in *Six6* null retinas (Figure 4C), and Six6 was unaffected in conditional *Six3* null retinas either (data not shown). Vsx2, a marker for both NR progenitors and CM progenitors (Horsford et al., 2005; Kuwahara et al., 2015), was unaffected in either *Six3*$^{F/F}$;*α-Cre* retinas or *Six3*$^{F/F}$;*Six6*$^{-/-}$ retinas (Figures 4E–4G) but was drastically affected in DKO retinas (Figure 4H). Although Six3 was deleted in both far- and mid-peripheral regions in DKO retinas (Figure 4D), Vsx2 was absent in mid-peripheral regions but remained in far-peripheral regions (Figure 4H). Vsx2 expression at the far-peripheral regions in DKO retinas likely represented its expression in the CM, since additional CM markers were also present (see also Figures 4T and 4X). The loss of Vsx2 expression in the mid-peripheral regions indicated defective NR progenitors in DKO retinas. Consistently, multi-lineage retinal differentiation was severely affected. Otx2, a transcription factor required for photoreceptor, bipolar, and horizontal cell development (Nishida et al., 2003; Sato et al., 2007), was unaffected in either *Six3*$^{F/F}$;*α-Cre* retinas or *Six3*$^{F/F}$;*Six6*$^{-/-}$ retinas (Figure 4I–4K) but was nearly absent at both far- and mid-peripheral regions of DKO retinas (Figures 4A, 4L, and 4L’), indicating severe defects in photoreceptor, bipolar, and horizontal cell differentiation. In addition, retinal ganglion cell differentiation was also severely affected. Shh is expressed in retinal ganglion cells and is required for retinal laminar structure (Wang et al., 2002). Shh was unaffected in either *Six3*$^{F/F}$; *α-Cre* retinas or *Six3*$^{F/F}$;*Six6*$^{-/-}$ retinas (Figures S5A–S5C) but was nearly absent in far-peripheral regions and significantly reduced in mid-peripheral regions in DKO retinas (Figures S5A and S5D). Severe reduction in Shh

Author Manuscript Author Manuscript Author Manuscript Author Manuscript

expression (Figure S5D) was consistent with the absence of Gli1 (Figure 2P), a target of Shh signaling (Lee et al., 1997). Defects in retinal ganglion cell differentiation were further confirmed by severe reduction of Pou4f2 at both expression levels and numbers at E14.5 and E15.5 (Figures 3H, S5H, and S5H'). In contrast, amacrine cell differentiation was relatively unaffected in mid-peripheral regions of DKO retinas. Neurod1, a bHLH transcription factor involved in amacrine cell differentiation (Inoue et al., 2002; Marquardt et al., 2001), was expressed in NR progenitors but not in CM progenitors in the control, *Six3*$^{F/F}$; *α-Cre*, or *Six3*$^{F/F}$;*Six6*$^{-/-}$ retinas (Figures 4M–4O). In DKO retinas, Neurod1 was absent or significantly reduced in far-peripheral regions but remained in mid-peripheral regions with disrupted stratification (Figure 4P). Similar expression changes were found for Foxn4 (Figures S5I–S5L), a transcription factor both necessary and sufficient for amacrine cell fate but nonredundantly required for horizontal cells (Li et al., 2004). In DKO retinas, the absence or reduction of Otx2, Neurod1, Shh, Pou4f2, and Foxn4 in the far-peripheral regions (Figures 4L, 4P, S5D, S5H, and S5L) confirmed the loss of NR identity; the presence of Neurod1 and Foxn4 (Figures 4P and S5L) but the absence or reduction of Vsx2, Otx2, and Shh (Figures 4H, 4L, and S5D) in the mid-peripheral regions indicates differentiation defects in multiple lineages but amacrine cells.

The loss of NR identity in far-peripheral regions of DKO retinas could be accompanied by a gain of CM marker expression, as indicated by upregulated CM marker p57 (Figure S2P). Activation of Wnt/β-catenin signaling is necessary and sufficient for CM development in mice (Cho and Cepko, 2006; Esteve et al., 2011; Fotaki et al., 2013; Heavner et al., 2014; Liu et al., 2007). Axin2, a readout of Wnt/β-catenin signaling (Jho et al., 2002), was very weakly expressed in the CM in the control retinas (Figure 4Q) and unaffected in either *Six3*$^{F/F}$;*α-Cre* retinas or *Six3*$^{F/F}$; *Six6*$^{-/-}$ retinas (Figures 4R and 4S) but was ectopically upregulated in DKO retinas (Figure 4T). Consistently, Otx1, a CM marker stimulated by Wnt/β-catenin signaling (Liu et al., 2007), was unaffected in either *Six3*$^{F/F}$;*α-Cre* retinas or *Six3*$^{F/F}$;*Six6*$^{-/-}$ retinas (Figures 4U–4W) but ectopically upregulated in DKO retinas (Figures 4U and 4X). Interestingly, Otx1 upregulation was mostly restricted to the far-peripheral regions (Figure 4X) where Neuod1 and Foxn4 were largely absent (Figures 4P and S5L). In *Six3*$^{F/F}$; *α-Cre* retinas, Cre expression was widely expressed in the peripheral retinas at E12.5 but restricted to CMs at E15.5 (Figures S5Q and S5R). In DKO retinas, however, Cre expression was continuously found in wide areas at E15.5 (Figures S5S and S5T), consistent with the expression pattern of GFP (Cre-IRESGFP) at E14.5 (Figures 1J and 1K). Importantly, upregulated Otx1 was found in Cre-positive Six3-neganive cells in which Axin2 was also upregulated but NR markers Otx2, Shh, and Pou4f2 were absent or severely reduced (Figures 4D, 4L, 4P, 4T, and 4X; Figures S5D, S5H, S5L, S5R, and S5T), indicating that ectopic Otx1 expression was accompanied by ectopic upregulation of Wnt signaling and loss of NR identity in DKO cell population. Collectively, DKO retinal cells in far-peripheral regions gained CM cell fate at the cost of NR identity, whereas DKO retinal cells in mid-peripheral regions maintained NR fate but lost multipotency.

Author Manuscript Author Manuscript Author Manuscript Author Manuscript

Postnatal DKO Retinas Lack a Laminar Structure and Comprise Only a Subpopulation of Amacrine Cells and Infiltrated Astrocytes

To determine the outcomes of defective retinal differentiation in DKO retinas, we analyzed retinal cell types on postnatal day 11, a stage when retinal cell fate determination has completed. Six3 was efficiently deleted (Figures 5A–5F). Retinal cell types were unaffected in *Six3*$^{F/F}$;*α-Cre*;*Six6*$^{+/-}$ retinas, although *Six3*$^{F/F}$;*α-Cre*;*Six6*$^{+/-}$ retinas were thinner. In DKO retinas, however, Rho and cone arrestin, markers for rod and cone photoreceptors, respectively, were absent (Figures 5F and 5I), indicating the absence of photoreceptors in DKO retinas. Similarly, bipolar, horizontal, and photoreceptor marker Otx2, retinal ganglion cell marker Pou4f2, and horizontal cell marker neurofilament (medium polypeptide) were absent in DKO retinas (Figures 5L, 5O, and 5R). In areas where residual Six3 remained in DKO retinas, Rho and Otx2 remained (arrows in Figures 5F and 5L), indicating that the phenotypes highly depended on *Six3* deletion. In contrast, amacrine cell markers syntaxin and Pax6 were widely expressed in DKOs (Figures 5I and 5L). Furthermore, amacrine cell markers Calretinin, GAD65, GABA, and TH were widely found (Figures S6D, S6H, S6L, and S6P), but GlyT1 and ChAT were rarely found in DKO retinas (Figures S6T and S6X), indicating only a subpopulation of amacrine cells persisted in postnatal DKO retinas. In addition to the defects in retinal neurons, Müller glia was absent in DKO retinas, as indicated by the absence of Lhx2 and Glul (Figures S7A–S7D). Furthermore, DKO retinas were widely infiltrated by Gfap-positive astrocytes (Figures S7E–S7H). Collectively, postnatal DKO retinas lack a laminar structure and comprise only a subpopulation of amacrine cells and infiltrated astrocytes, confirming the defects in multi-lineage retinal differentiation.

The Gene Set Jointly Regulated by Six3 and Six6 Highly Overlaps with the Gene Networks Regulated by WNT3A, CTNNB1, POU4F2, or SOX2

We sought to identify the gene set jointly regulated by Six3 and Six6 in NR progenitors using RNA-seq assay. The whole DKO retinas driven by *α-Cre* are not ideal for bulk RNA-seq, since the differentially expressed genes (DEGs) in the Cre-positive peripheral NR will be averaged out by the gene expression in the Cre-negative central NR. To overcome the drawback of *α-Cre*, we utilized *CAGGCre-ER*^{TM} to ubiquitously delete *Six3* at E10.5 to generate E13.5 *Six3*$^{F/F}$;*CAGGCre-ER*^{TM};*Six6*$^{-/-}$ compound null retinas. Notably, compound *Six3* and *Six6* deletion driven by either *CAGGCre-ER*^{TM} or *α-Cre* led to consistent phenotypes (data not shown). Transcriptome comparison between three DKOs and three wild-types (WTs) using DESeq2 identified 800 DEGs in E13.5 DKOs (Table S1, padj < 0.05). Expression changes in DEGs were highly correlated with the efficiency of *Six3* deletion, since relatively less *Six3* deletion in one DKO sample (DKO_rh021) caused low levels of expression changes (Figure 6A; data not shown). Visual inspection of the plotted heatmap found that one WT sample slightly deviated from the other two in the WT group (Figure 6A). Therefore, we performed an additional transcriptome comparison between two DKO samples and two WT samples after removing the deviated ones, resulting in 1152 DEGs (padj < 0.05). Combining the two lists of DEGs, 1321 DEGs in total were identified in E13.5 DKO retinas driven by *CAGGCre-ER*^{TM} (Table S2, padj < 0.05), covering 15 out of 24 previously identified DEGs in E14.5–15.5 DKO retinas driven by *α-Cre* (Figures 2, 3, 4, 6A, and S2–S5). The list in Table S1 is stringent, whereas the list in Table S2 identifies

Author Manuscript Author Manuscript Author Manuscript Author Manuscript

additional DEGs, e.g., Pou4f2 and Neurod1 as confirmed in Figure 3H and Figure 4P, respectively, indicating a value of performing the second comparison. Importantly, RNA-seq assay identified additional DEGs that were functionally relevant, e.g., upregulated *Fzd1*, *Wnt3a*, *Wnt16*, and *Cdon*; all the four DEGs were validated in DKO retinas (Figures 6A, 6C–6N, and 7A–7D). In addition, Wnt3a, Fzd1, Cdon, Otx1, and Wnt16 were closely clustered in the heatmap, suggesting their close functional relationship. Furthermore, upregulation of Fzd1, Axin2, Otx1, Wnt3a, and Wnt16 was found as early as E12.5 (data not shown), a stage 1 day after conditional Six3 deletion (Figures 1D and 1E), indicating the upregulation of Wnt/β-catenin signaling and CM markers was an early response to Six3 and Six6 dual deletion. When Six3KOs or Six6KOs were compared to WTs, only 16 and 68 DEGs were identified, respectively (Tables S3 and S4, padj < 0.05). Collectively, our RNA-seq not only confirms most known DEGs but also identifies additional DEGs in DKO retinas.

To elucidate the gene regulatory network (GRN) jointly regulated by Six3 and Six6, we performed Ingenuity Pathway Analysis (IPA) (Krämer et al., 2014) using a stringent list of DEGs in DKOs as follows: 333 analysis-ready DEGs resulting from the comparison between three DKOs and three WTs using padj < 0.05 and |log2FC| > 1 as a cutoff. Upstream regulator analysis identified the top five upstream regulators, WNT3A, POU4F2, CTNNB1, SOX2, and beta-estradiol (Figure 6B), indicating that the gene set jointly regulated by Six3 and Six6 highly overlapped with the GRNs regulated by WNT3A, POU4F2, CTNNB1, or SOX2. In the 333 analysis-ready DEGs, 116 and 132 DEGs were in WNT3A- and CTNNB1-regulated GRNs, respectively, suggesting the involvement of Wnt/β-catenin signaling under the regulation of Six3 and Six6 joint functions. Consistently, KEGG pathway analysis indicated that DEGs in Wnt signaling pathway had the highest percentage (data not shown). In support of the upstream regulator analysis, several components of Wnt/β-catenin signaling, i.e., Axin2, Fzd1, Wnt3a, and Wnt16, were significantly upregulated (Figures 4Q–4T and 6C–6N), whereas Sox2 and Pou4f2 were downregulated in DKO retinas (Figures 2E–2H, 3E–3H, and S5E–S5H). Interestingly, Axin2 and Fzd1 were upregulated more widely than Wnt3a and Wnt16 (Figures 4T, 6F, 6J, and 6N), indicating complex regulation of Wnt/β-catenin signaling by Six3 and Six6 joint functions. IPA also identified the following top five molecular and cellular functions of the DEGs: cellular movement, cellular development, cellular growth and proliferation, cell morphology, cell death, and cell survival (Figure 6B), which were highly consistent with marker analysis (Figures 2, 3, 4, and S2–S5). Collectively, transcriptome profiling of DKO retinas highly indicates that Six3 and Six6 jointly regulate a GRN involving Wnt/β-catenin signaling, Sox2, and Pou4f2 in retinal cell differentiation.

Stimulation of Wnt/β-Catenin Signaling by Either Wnt-3a or a GSK3β Inhibitor Promotes CM Cell Fate at the Cost of NR Identity at the Periphery of Mouse Eyecups

To determine the functional consequences of upregulated Wnt3a, Wnt16, and Wnt/β-catenin signaling in DKO retinas, we examined the CM in mouse eyecup cultures supplemented with recombinant Wnt-3a, Wnt-16b, or a GSK3β inhibitor CHIR99021. Cdon, a CM marker (Bélanger et al., 2017), was significantly upregulated in DKO retinas (Figures 6A and7A–7D). In the mouse eyecup cultures treated with vehicles, the CM was found in Cdon-positive

Author Manuscript Author Manuscript Author Manuscript Author Manuscript

and Tubb3-negative areas (Figure 7E). In mouse eyecups treated with Wnt-16b, the CM size was comparable to that in the vehicle controls (Figure 7F). In the eyecups treated by Wnt-3a, however, the length of CM (Cdon-positive Tubb3-negative) was much longer than that in the vehicle controls (Figures 7E and 7G). Similarly, the CM was also longer in the eyecups treated with a GSK3β inhibitor CHIR99021 (Figures 7E and 7H). Interestingly, in the eyecups treated with either Wnt-3a or CHIR99021, CM expansion was restricted to the periphery of mouse eyecups (Figures 7E, 7G, and 7H). In the expanded CM, Six3 expression was reduced (data not shown). Collectively, activation of Wnt/β-catenin signaling by either Wnt-3a or a GSK3β inhibitor promotes CM cell fate at the cost of NR identity at the periphery of mouse eyecups.

DISCUSSION

Through molecular characterization of DKO retinas, transcriptome profiling, IPA, and manipulation of Wnt/β-catenin signaling in mouse eyecup cultures, we have demonstrated that Six3 and Six6 together are essential for maintaining a pool of multipotent NR progenitors at least through two molecular mechanisms. Six3 and Six6 jointly suppress Wnt/β-catenin signaling, since an inverse relationship between Six3/Six6 joint functions and Wnt/β-catenin signaling was found. Six3 and Six6 together also maintain the expression of multiple retinogenic regulators, including Sox2, Notch1, Hes5, Shh, Gli1, bHLH transcription factors, Fgf15, Pou4f2, and Otx2. Thus, Six3 and Six6 are jointly required for the maintenance of multipotent NR progenitors through both negative and positive regulation.

Six3, together with Six6 at later stages, is an essential a cell-fate determinant to protect NR progenitors from adopting alternative cell fates at least through suppressing Wnt/β-catenin signaling. Six3 initially represses Wnt1 to promote rostral forebrain and eye field precursors against caudal forebrain cell fate (Lagutin et al., 2003). Next, Six3 represses Wnt8b to promote NR progenitors against RPE progenitor cell fate (Liu et al., 2010). Here, we have demonstrated that Six3 and Six6 together suppress Wnt/β-catenin signaling to protect multipotent NR progenitors against CM progenitor cell fate, because (1) Wnt3a, Fzd1, Axin2, and Wnt16 were ectopically upregulated in DKO retinas; (2) the gene set jointly regulated by Six3 and Six6 highly overlapped with the GRNs regulated by WNT3A or CTNNB1; and (3) stimulation of Wnt/β-catenin signaling by either Wnt-3a or a GSKβ inhibitor promoted CM progenitors at the cost of NR identity at the periphery of mouse eyecups. In DKO retinas, Fzd1 and Axin2 were upregulated widely, whereas Wnt3a and Wnt16 were upregulated in patches, suggesting complex suppression of Wnt/β-catenin signaling by Six3/Six6 joint functions. Simultaneous upregulation of Fzd1 and Wnt3a in DKO retinas would synergize to stimulate Wnt/β-catenin signaling, since Wnt3a interacts with Fzd1 in signal transduction (Voloshanenko et al., 2017). The association between upregulated Wnt/β-catenin signaling and CM markers in DKO retinas is well consistent with the model that activation of Wnt/β-catenin signaling is necessary and sufficient for CM development in chicks and mice (Cho and Cepko, 2006; Esteve et al., 2011; Fotaki et al., 2013; Heavner et al., 2014; Kinoshita et al., 2016; Kubo et al., 2003; Liu et al., 2007). Importantly, only far-peripheral NR adopted CM cell fate at the cost of NR identity in response to either joint *Six3/Six6* deletion *in vivo* or stimulation of Wnt/β-catenin signaling

Author Manuscript Author Manuscript Author Manuscript Author Manuscript

in vitro. Relatedly, Wnt/β-catenin signaling and CM specification were normally found at the most-peripheral NR where both Six3 and Six6 were weakly expressed, and stimulation of Wnt/β-catenin signaling in mouse eyecups did not affect Six3 expression in central NR. Collectively, low levels of Six3 and Six6 permit Wnt/β-catenin signaling resulting in CM specification at the most-peripheral NR, whereas high levels of Six3 and Six6 jointly suppress Wnt/β-catenin signaling to protect multipotent NR progenitors against CM progenitor cell fate in the central NR.

Six3 and Six6 together constitute an additional regulatory program required for the multipotency of NR progenitors. Previous studies demonstrate that Pax6, Sufu, and Sox2 also regulate multipotent NR progenitors (Cwinn et al., 2011; Heavner et al., 2014; Marquardt et al., 2001; Matsushima et al., 2011; Taranova et al., 2006). Although amacrine cells are exclusively found in *Pax6* null, *Sufu* null, and DKO retinas at postnatal stages, the positions of these amacrine cells and the underlying molecular mechanisms differ in the mutant mice. In *Pax6* null and *Sufu* null retinas, amacrine cells were found in far-peripheral regions (Cwinn et al., 2011; Marquardt et al., 2001), whereas amacrine cells were found in mid-peripheral regions of DKO retinas. In embryonic DKO retinas, Pax6 expression remained and Gli1 expression was nearly absent, indicating that the phenotypes in DKO retinas were not mediated by either Pax6 loss as seen in *Pax6* null retinas or by increased Gli1 as seen in *Sufu* null retinas. Reduced Sox2 expression in DKO retinas contributed to the downregulation of NR progenitor markers, e.g., Notch1, Hes5, and Gli1, but amacrine cells were found in DKO retinas but not in *Sox2* null retinas, indicating that the pathways regulated by Six3/Six6 joint functions and Sox2 differ in some aspects. In embryonic DKO retinas, the severe reduction or absence of Atoh7 (Wang et al., 2001), Pou4f2 (Gan et al., 1996), and Shh/Gli1 (Wang et al., 2002) resulted in defects in retinal ganglion cell differentiation; the loss of Otx2 (Nishida et al., 2003; Sato et al., 2007) disrupted photoreceptor, bipolar, and horizontal cell differentiation; the sustained expression of Neurod1 (Inoue et al., 2002) and Foxn4 (Li et al., 2004) suggested largely unaffected amacrine cell differentiation. Cell type analysis in postnatal DKO retinas confirmed those embryonic alterations. The lack of a laminar structure in DKO retinas is probably due to apical junction defects mediated by upregulated Wnt/β-catenin signaling, since continuous Wnt/β-catenin signaling leads to neuroepithelial aberrations via the accumulation of aPKC at the apical pole (Herrera et al., 2014). Collectively, Six3 and Six6 jointly regulate the expression of multiple retinogenic factors essential for the multipotency of NR progenitors.

CM expansion at the far periphery and multipotency loss at the mid periphery in DKO retinas imply intrinsic differences in NR progenitors along peripheral-central axis. Similarly, in mouse eyecup cultures, the CM was expanded only at the periphery when Wnt/β-catenin signaling was stimulated by either Wnt-3a or GSK3β inhibitor CHIR99021. These findings indicate that NR progenitors at the periphery, but not at the center, had the competence to adopt CM cell fate at the expense of NR progenitors in response to either simultaneous *Six3* and *Six6* deletion or activated Wnt/β-catenin signaling. Moving centrally, NR progenitors maintained neural identity but lost multipotency when both *Six3* and *Six6* were deleted. Consistent with our findings, a divergence of NR progenitors in response to *Pax6* deletion (using α-Cre) was described (Oron-Karni et al., 2008). Further analysis will determine how the region-specific phenotypes formed in DKO retinas.

Author Manuscript Author Manuscript Author Manuscript Author Manuscript

Loss-of-function studies described previously (Liu and Cvekl, 2017) and here indicate that Six3 and Six6 jointly regulate retinal differentiation. Given that Six3 and Six6 are largely co-localized and display high similarity in their homeodomain and six domains, Six3 and Six6 may share gene targets and/or interacting proteins. If true, the lack of overt phenotypes in either *Six3* null (deletion at E9.5–10.5) or *Six6* null retinas is due to functional compensation, whereas the ablation of NR specification caused by *Six3* deletion at E8.0–8.5 (Liu et al., 2010) is because of a lack of compensation due to a late onset of Six6 expression. It will be interesting to determine how much Six6 will compensate for the loss of Six3 when *Six6* is knocked into *Six3* locus. Alternatively, Six3 and Six6 may have unique gene targets and/or interacting proteins, and their downstream effectors synergize in retinal cell differentiation. Since the exact phenotypes in DKO retinas have not been described in any single mutant mouse retinas, it is conceivable that Six3 and Six6 jointly regulate unknown or multiple factors in retinal cell differentiation, which makes it difficult to pinpoint candidates for testing. Further studies will elucidate how Six3 and Six6 together suppress Wnt/β-catenin signaling but promote retinogenic factors to maintain multipotent NR progenitors in mouse embryonic retinas.

STAR★METHODS

CONTACT FOR REAGENT AND RESOURCE SHARING

Further information and requests for resources and reagents generated in this study should be directed to and will be fulfilled by the Lead Contact, Wei Liu (Wei.Liu@einstein.yu.edu).

EXPERIMENTAL MODEL AND SUBJECT DETAILS

Mice—The mice were housed in the Animal Institute in Albert Einstein College of Medicine using a standard husbandry. $Six3^{F/F}$ (Liu et al., 2006), $Six6^{+/-}$ (Li et al., 2002), *Pax6 α-Cre* mice (Marquardt et al., 2001), and $CAGGCre\text{-}ER^{TM}$ mice (Hayashi and McMahon, 2002) were maintained in the NMRI background and genotyped using methods as previously described. $Six3^{F/F}$; *α-Cre* embryos and mice were generated by crossing female $Six3^{F/F}$ or $Six3^{F/+}$ mice with male $Six3^{F/+}$; *α-Cre* mice. $Six3^{F/F}$; *α-Cre*; $Six6^{-/-}$ embryos and mice were generated by crossing female $Six3^{F/F}$; $Six6^{+/-}$ mice with male $Six3^{F/F}$; *α-Cre*; $Six6^{+/-}$ mice. For the generation of $Six3^{F/F}$; $CAGGCre\text{-}ER^{TM}$; $Six6^{-/-}$ embryos, $Six3^{F/F}$; $Six6^{+/-}$ pregnant dams crossed with male $Six3^{F/F}$; $CAGGCre\text{-}ER^{TM}$; $Six6^{+/-}$ mice were administered with Tamoxifen using intraperitoneal injections (3 mg in corn oil per mouse each time) on E10.5 and E11.5.

Embryos and postnatal mice with the same genotype, the same age were allocated into experimental groups. Retinal phenotypes in DKO retinas were always correlated to the efficiency of conditional Six3-deletion. $Six3^{F/F}$ retinas, *α-Cre* retinas, and $Six3^{F/F}$; $Six6^{+/-}$ retinas were indistinguishable in the assays described here, and were used as controls for DKO retinas. Littermates were used when possible. The age of embryos and mice were reported in each analysis. Since gender as variables for retinal cell differentiation have never been reported in literature, embryos and mice with both genders were used indistinguishably in our studies. A minimum of three embryos in each group was analyzed. Animal

Author Manuscript Author Manuscript Author Manuscript Author Manuscript

experiments were approved by the Animal Care and Use Committees in Albert Einstein College of Medicine.

METHOD DETAILS

Immunohistochemistry and *in situ* hybridization—Embryos were fixed in 4% paraformaldehyde overnight at 4°C, cryopreserved in 30% sucrose, embedded in OCT (Tissue Tek), and stored in −80°C until further use. Transverse frozen sections (10 μm) were used for immunohistochemistry and *in situ* hybridization using standard protocols. For immunohistochemistry, antigen was first recognized by primary antibodies, and then visualized using Alexa Fluor 488- or Cy3.5-conjugated secondary antibodies under Zeiss AxioObserver Z1 microscope. These primary antibodies are used: Choline Acetyltransferase (Millipore AB144P, 1:400), Cone Arrestin (Millipore AB15282, 1:5000), GAD65 (Fisher Scientific BDB559931, 1:200), GABA (Sigma A2052, 1:100), GFAP (Sigma G9269, 1:4000), Glul (also known as glutamine synthetase, BD Bioscience #610517, 1:500), Glycine Transporter 1 (Millipore AB1770, 1:5000), Laminin-1 A&B (Millipore MAB1904, 1:500), Lhx2 (Santa Cruz sc-19344, 1:1600), Neurofilament M (Millipore AB1987, 1:500), Otx2 (R&D Systems AF1979, 1:1500), p27 (Santa Cruz sc776, 1:200), Pax6 (Covance #PRB-278P, 1:500), pH3 (Upstate #06–570, 1:250), Prkcz (also known as PKC ζ, Santa Cruz sc-216, 1:400), Pou4f2 (also known as Brn3b, Santa Cruz sc-6026, 1:100), Rho (Abcam #ab98887, 1:500), Six3 (Rockland #600–401-A26, 1:500), Sox2 (Chemicon #AB5770, 1:800), Syntaxin (Sigma #S0664, 1:1000), Tyrosine Hydroxylase (Millipore AB152, 1:400), Tubb3 (BabCO #MMS435P clone Tuj1, 1:500), and Vsx2 (Abcam #AB9016, 1:500).

To prepare DIG-labeled RNA probes for *in situ* hybridization, cDNA of mouse genes (Origene) were subcloned into pBluescript plasmid. The resulting template plasmids were linearized for antisense direction, and *in vitro* transcribed using DIG RNA Labeling Kit (Roche #11277073910). Template plasmids were also requested from other laboratories. The *in situ* hybridization probes are: Ascl1 (Xba/SP6), Atoh7 (Asc1/T7), Axin2 (NotI/T3), CyclinD1 (NarI/T7), FGF15 (NotI/T7), Foxn4 (BglII/T3), Fzd5 (NotI/T7), Fzd1 (BamHI/T3), Gli1 (NotI/T3), Hes1 (EcoRI/T3), Hes5 (BamHI/T7), Neurod1 (XhoI/T7), Neuod4 (XhoI/T3), Neurog2 (NotI/T7), Notch1 (Cla/T7), Otx1 (NdeI/T7), p57 (SalI/T3), Shh (HindIII/T3), Six6 (XbaI/T7), Wnt3a (EcoRI/T3), and Wnt16 (EcoRI/T3).

Eyecup cultures—E12.5 eyecups containing the neuroretina and lens were dissected out from wild-type NMRI embryos, rinsed, and placed into a 24-well plate on an orbital shaker for 6-day culture (37°C, 5% CO2). The culture medium (DMEM/F12, 8% FBS, 2% B27, and PenStrep) was supplemented with recombinant human Wnt-3a (250 ng/mL, R&D Systems 5036-WN-010), Wnt-16b (250 ng/ml, R&D Systems 7790-WN-025), a GSK3β inhibitor CHIR99021 (3 μM, TOCRIS), or vehicles (0.1% BSA or DMSO), with a medium change on day 3. After the culture, the eyecups were fixed in 4% PFA in PBS for 2 hr at room temperature, and then processed for cryosections. Three eyecups in each group were analyzed.

Author Manuscript Author Manuscript Author Manuscript Author Manuscript

Transcriptome profiling using RNA-seq—*Six3*$^{F/F}$; *Six6*$^{+/-}$ dams crossed with *Six3*$^{F/F}$; *CAGGCre-ER*^{TM}; *Six6*$^{+/-}$ male mice were intraperitoneally injected with Tamoxifen (0.15 mL of 20 mg/mL stock solution in corn oil per mouse for each injection) at E10.5 (approximately 2pm) and E11.5 (approximately 9 am). One pair of retinas from each E13.5 embryo (noon) were dissected out in ice-cold PBS, rinsed, and then stored individually in 100 μL of RNAlater (Ambion) in an Eppendorf tube overnight at 4 °C. After RNAlater was removed, the samples were stored at −80 °C until purification.

The retinas with the following genotypes were used for RNA isolation using the RNeasy Micro Kit (QIAGEN) after genotyping: 1) WT (*Six3*$^{F/F}$; *Six6*$^{+/+}$); 2) Six3KO (*Six3*$^{F/F}$; *CAGGCre-ER*^{TM}); 3) Six6KO (*Six3*$^{F/F}$; *Six6*$^{-/-}$); 4) DKO (*Six3*$^{F/F}$; *CAGGCre-ER*^{TM}; *Six6*$^{-/-}$). For each genotype group, RNA from one pair of retinas was individually isolated, with three pairs of retinas in total. The retinas were homogenized with an electric pellet pestle motor in 500uL of Qiazol. Total RNA was purified using micro columns, treated with RNase-free DNase set (QIAGEN), and eluted in 14uL of RNase-free water. The quantity and quality of RNA were verified using Qubit fluorometer (Thermo Fisher Scientific) and Bioanalyzer (Agilent Genomics), respectively.

Total RNA (181.2–792 ng for each sample, RIN > 9) was used for library preparation using KAPA RNA HyperPrep Kit with RiboErase (HMR) (Kapa Biosystems). Sequencing was run on Illumina HiSeq 2500 in 100-bp single-end high-output mode in the Einstein Epi-genomics Core Facility. About 30 million reads were generated for each sample. Each genotype group initially had three biological replicates, but one Six6KO replicate was later removed due to over duplication. After trimming adaptor with Trim Galore (v. 0.3.7), RNA-seq reads were aligned back to mouse genome mm10 using Tophat (v. 2.0.13) (Trapnell et al., 2009). The number of reads mapped back to each gene was calculated with HTseq (v. 0.6.1) (Anders et al., 2015) using Refseq gene annotation (downloaded from the UCSC genome browser in 03/17). The Cuffdiff in Cufflinks package (v. 2.2.1) (Trapnell et al., 2010) was used to generate FPKM values. We focused on 13498 genes that have FPKM value > 1 in at least one of samples. Deseq2 (Love et al., 2014) was used to determine the differentially expressed genes (DEGs) with FDR (padj) less than 0.05 as a cutoff unless it is stated otherwise. For visualization, heatmap was plotted using the normalized counts generated by DESeq2. For functional annotation of the DEGs from the comparison between three DKOs and three WTs (padj < 0.05, |log2FC| > 1, 333 analysis-ready DEGs), Ingenuity Pathway Analysis (Krämer et al., 2014) was used.

QUANTIFICATION AND STATISTICAL ANALYSIS

Cell counting—Transverse frozen sections (10 μm) at levels close to optic nerve were used for either immunostaining or TUNEL assay (ApoTag Kit, Chemicon). The numbers of positive cells (pH3 positive cells, TUNEL positive cells, Otx2 positive cells, and Pou4f2 positive cells) in the marked peripheral areas were counted, and the lengths of the marked apical surface were measured using ImageJ (Schneider et al., 2012). The density of positive cells was expressed as the number of positive cells per 1 mm of marked apical length per section. Retinas from three wild-type and three DKO embryos were used for cell counting.

Author Manuscript Author Manuscript Author Manuscript Author Manuscript

Statistical analysis—*p value* of Student's t test (two tailed distribution, equal variance), determined by Microsoft Excel for Mac 2011 software, was used to compare the two means for wild-type and DKO retinas in the density of pH3 positive cells, TUNEL positive cells, Otx2 positive cells, and Pou4f2 positive cells, with $p < 0.001$ considered statistical significance.

DATA AND SOFTWARE AVAILABILITY

Data deposit—The accession number for the RNA-seq data reported in this paper is GEO: GSE115258. (https://www.ncbi.nlm.nih.gov/geo).

Software availability—The software used for RNA-seq analysis in this study is available using the URLs listed in Key Resources Table.

Supplementary Material

Refer to Web version on PubMed Central for supplementary material.

ACKNOWLEDGMENTS

We thank Drs. G. Oliver for generous support, M.G. Rosenfeld and X. Li for the *Six6* mice, and V. Wallace, T. Glaser, M. Xiang, and X. Mu for probes. We thank Armand Mbanya for subcloning a few plasmids. We thank the Epigenomics Shared Facility at AECOM for sequencing. This work was partially supported by grants from the National Institutes of Health, United States (EY022645 to W.L., EY012200 to A.C.), Research to Prevent Blindness, United States (unrestricted to the Department of Ophthalmology and Visual Sciences at AECOM), and the Joseph Alexander Foundation (to R. Chuck). R.D. is supported by training grant T32GM007288.

REFERENCES

Anders S, Pyl PT, and Huber W (2015). HTSeq–a Python framework to work with high-throughput sequencing data. Bioinformatics 31, 166–169. [PubMed: 25260700]

Bélanger MC, Robert B, and Cayouette M (2017). Msx1-positive progenitors in the retinal ciliary margin give rise to both neural and non-neural progenies in mammals. Dev. Cell 40, 137–150. [PubMed: 28011038]

Brown NL, Kanekar S, Vetter ML, Tucker PK, Gemza DL, and Glaser T (1998). Math5 encodes a murine basic helix-loop-helix transcription factor expressed during early stages of retinal neurogenesis. Development 125, 4821–4833. [PubMed: 9806930]

Brzezinski JA, 4th, Kim EJ, Johnson JE, and Reh TA (2011). Ascl1 expression defines a subpopulation of lineage-restricted progenitors in the mammalian retina. Development 138, 3519–3531. [PubMed: 21771810]

Burns CJ, Zhang J, Brown EC, Van Bibber AM, Van Es J, Clevers H, Ishikawa TO, Taketo MM, Vetter ML, and Fuhrmann S (2008). Investigation of Frizzled-5 during embryonic neural development in mouse. Dev. Dyn 237, 1614–1626. [PubMed: 18489003]

Cepko C (2014). Intrinsically different retinal progenitor cells produce specific types of progeny. Nat. Rev. Neurosci 15, 615–627. [PubMed: 25096185]

Cho SH, and Cepko CL (2006). Wnt2b/beta-catenin-mediated canonical Wnt signaling determines the peripheral fates of the chick eye. Development 133, 3167–3177. [PubMed: 16854977]

Cwinn MA, Mazerolle C, McNeill B, Ringuette R, Thurig S, Hui CC, and Wallace VA (2011). Suppressor of fused is required to maintain the multipotency of neural progenitor cells in the retina. J. Neurosci 31, 5169–5180. [PubMed: 21451052]

Dias da Silva MR, Tiffin N, Mima T, Mikawa T, and Hyer J (2007). FGF-mediated induction of ciliary body tissue in the chick eye. Dev. Biol 304, 272–285. [PubMed: 17275804]

Author Manuscript Author Manuscript Author Manuscript Author Manuscript

Esteve P, Sandonìs A, Ibañez C, Shimono A, Guerrero I, and Bovolenta P (2011). Secreted frizzled-related proteins are required for Wnt/β-catenin signalling activation in the vertebrate optic cup. Development 138, 4179–4184. [PubMed: 21896628]

Feng L, Xie ZH, Ding Q, Xie X, Libby RT, and Gan L (2010). MATH5 controls the acquisition of multiple retinal cell fates. Mol. Brain 3, 36. [PubMed: 21087508]

Fotaki V, Smith R, Pratt T, and Price DJ (2013). Foxg1 is required to limit the formation of ciliary margin tissue and Wnt/β-catenin signalling in the developing nasal retina of the mouse. Dev. Biol 380, 299–313. [PubMed: 23624311]

Gan L, Xiang M, Zhou L, Wagner DS, Klein WH, and Nathans J (1996). POU domain factor Brn-3b is required for the development of a large set of retinal ganglion cells. Proc. Natl. Acad. Sci. USA 93, 3920–3925. [PubMed: 8632990]

Hayashi S, and McMahon AP (2002). Efficient recombination in diverse tissues by a tamoxifen-inducible form of Cre: a tool for temporally regulated gene activation/inactivation in the mouse. Dev. Biol 244, 305–318. [PubMed: 11944939]

Heavner WE, Andoniadou CL, and Pevny LH (2014). Establishment of the neurogenic boundary of the mouse retina requires cooperation of SOX2 and WNT signaling. Neural Dev. 9, 27. [PubMed: 25488119]

Herrera A, Saade M, Menendez A, Marti E, and Pons S (2014). Sustained Wnt/β-catenin signalling causes neuroepithelial aberrations through the accumulation of aPKC at the apical pole. Nat. Commun 5, 4168. [PubMed: 24942669]

Horsford DJ, Nguyen MT, Sellar GC, Kothary R, Arnheiter H, and McInnes RR (2005). Chx10 repression of Mitf is required for the maintenance of mammalian neuroretinal identity. Development 132, 177–187. [PubMed: 15576400]

Inoue T, Hojo M, Bessho Y, Tano Y, Lee JE, and Kageyama R (2002). Math3 and NeuroD regulate amacrine cell fate specification in the retina. Development 129, 831–842. [PubMed: 11861467]

Jean D, Bernier G, and Gruss P (1999). Six6 (Optx2) is a novel murine Six3-related homeobox gene that demarcates the presumptive pituitary/hypothalamic axis and the ventral optic stalk. Mech. Dev 84, 31–40. [PubMed: 10473118]

Jho EH, Zhang T, Domon C, Joo CK, Freund JN, and Costantini F (2002). Wnt/beta-catenin/Tcf signaling induces the transcription of Axin2, a negative regulator of the signaling pathway. Mol. Cell. Biol 22, 1172–1183. [PubMed: 11809808]

Kinoshita H, Suzuma K, Kaneko J, Mandai M, Kitaoka T, and Takahashi M (2016). Induction of functional 3D ciliary epithelium-like structure from mouse induced pluripotent stem cells. Invest. Ophthalmol. Vis. Sci 57, 153–161. [PubMed: 26780319]

Krämer A, Green J, Pollard J, Jr., and Tugendreich S (2014). Causal analysis approaches in Ingenuity Pathway Analysis. Bioinformatics 30, 523–530. [PubMed: 24336805]

Kubo F, Takeichi M, and Nakagawa S (2003). Wnt2b controls retinal cell differentiation at the ciliary marginal zone. Development 130, 587–598. [PubMed: 12490564]

Kuwahara A, Ozone C, Nakano T, Saito K, Eiraku M, and Sasai Y (2015). Generation of a ciliary margin-like stem cell niche from self-organizing human retinal tissue. Nat. Commun 6, 6286. [PubMed: 25695148]

Lagutin OV, Zhu CC, Kobayashi D, Topczewski J, Shimamura K, Puelles L, Russell HR, McKinnon PJ, Solnica-Krezel L, and Oliver G (2003). Six3 repression of Wnt signaling in the anterior neuroectoderm is essential for vertebrate forebrain development. Genes Dev. 17, 368–379. [PubMed: 12569128]

Lee J, Platt KA, Censullo P, and Ruiz i Altaba A (1997). Gli1 is a target of Sonic hedgehog that induces ventral neural tube development. Development 124, 2537–2552. [PubMed: 9216996]

Li X, Perissi V, Liu F, Rose DW, and Rosenfeld MG (2002). Tissue-specific regulation of retinal and pituitary precursor cell proliferation. Science 297, 1180–1183. [PubMed: 12130660]

Li S, Mo Z, Yang X, Price SM, Shen MM, and Xiang M (2004). Foxn4 controls the genesis of amacrine and horizontal cells by retinal progenitors. Neuron 43, 795–807. [PubMed: 15363391]

Liu W, and Cvekl A (2017). Six3 in a small population of progenitors at E8.5 is required for neuroretinal specification via regulating cell signaling and survival in mice. Dev. Biol 428, 164–175. [PubMed: 28579317]

Author Manuscript Author Manuscript Author Manuscript Author Manuscript

Liu W, Lagutin OV, Mende M, Streit A, and Oliver G (2006). Six3 activation of Pax6 expression is essential for mammalian lens induction and specification. EMBO J. 25, 5383–5395. [PubMed: 17066077]

Liu H, Xu S, Wang Y, Mazerolle C, Thurig S, Coles BL, Ren JC, Taketo MM, van der Kooy D, and Wallace VA (2007). Ciliary margin trans-differentiation from neural retina is controlled by canonical Wnt signaling. Dev. Biol 308, 54–67. [PubMed: 17574231]

Liu W, Lagutin O, Swindell E, Jamrich M, and Oliver G (2010). Neuroretina specification in mouse embryos requires Six3-mediated suppression of Wnt8b in the anterior neural plate. J. Clin. Invest 120, 3568–3577. [PubMed: 20890044]

Love MI, Huber W, and Anders S (2014). Moderated estimation of fold change and dispersion for RNA-seq data with DESeq2. Genome Biol. 15, 550. [PubMed: 25516281]

Lovicu FJ, and McAvoy JW (2005). Growth factor regulation of lens development. Dev. Biol 280, 1–14. [PubMed: 15766743]

Marcucci F, Murcia-Belmonte V, Wang Q, Coca Y, Ferreiro-Galve S, Kuwajima T, Khalid S, Ross ME, Mason C, and Herrera E (2016). The ciliary margin zone of the mammalian retina generates retinal ganglion cells. Cell Rep. 17, 3153–3164. [PubMed: 28009286]

Marquardt T, Ashery-Padan R, Andrejewski N, Scardigli R, Guillemot F, and Gruss P (2001). Pax6 is required for the multipotent state of retinal progenitor cells. Cell 105, 43–55. [PubMed: 11301001]

Martinez-Morales JR, Signore M, Acampora D, Simeone A, and Bovolenta P (2001). Otx genes are required for tissue specification in the developing eye. Development 128, 2019–2030. [PubMed: 11493524]

Matsushima D, Heavner W, and Pevny LH (2011). Combinatorial regulation of optic cup progenitor cell fate by SOX2 and PAX6. Development 138, 443–454. [PubMed: 21205789]

Nishida A, Furukawa A, Koike C, Tano Y, Aizawa S, Matsuo I, and Furukawa T (2003). Otx2 homeobox gene controls retinal photoreceptor cell fate and pineal gland development. Nat. Neurosci 6, 1255–1263. [PubMed: 14625556]

Oron-Karni V, Farhy C, Elgart M, Marquardt T, Remizova L, Yaron O, Xie Q, Cvekl A, and Ashery-Padan R (2008). Dual requirement for Pax6 in retinal progenitor cells. Development 135, 4037–4047. [PubMed: 19004853]

Sato S, Inoue T, Terada K, Matsuo I, Aizawa S, Tano Y, Fujikado T, and Furukawa T (2007). Dkk3-Cre BAC transgenic mouse line: a tool for highly efficient gene deletion in retinal progenitor cells. Genesis 45, 502–507. [PubMed: 17661397]

Schneider CA, Rasband WS, and Eliceiri KW (2012). NIH Image to ImageJ: 25 years of image analysis. Nat. Methods 9, 671–675. [PubMed: 22930834]

Taranova OV, Magness ST, Fagan BM, Wu Y, Surzenko N, Hutton SR, and Pevny LH (2006). SOX2 is a dose-dependent regulator of retinal neural progenitor competence. Genes Dev. 20, 1187–1202. [PubMed: 16651659]

Trapnell C, Pachter L, and Salzberg SL (2009). TopHat: discovering splice junctions with RNA-Seq. Bioinformatics 25, 1105–1111. [PubMed: 19289445]

Trapnell C, Williams BA, Pertea G, Mortazavi A, Kwan G, van Baren MJ, Salzberg SL, Wold BJ, and Pachter L (2010). Transcript assembly and quantification by RNA-Seq reveals unannotated transcripts and isoform switching during cell differentiation. Nat. Biotechnol 28, 511–515. [PubMed: 20436464]

Voloshanenko O, Gmach P, Winter J, Kranz D, and Boutros M (2017). Mapping of Wnt-Frizzled interactions by multiplex CRISPR targeting of receptor gene families. FASEB J. 31, 4832–4844. [PubMed: 28733458]

Wang SW, Kim BS, Ding K, Wang H, Sun D, Johnson RL, Klein WH, and Gan L (2001). Requirement for math5 in the development of retinal ganglion cells. Genes Dev. 15, 24–29. [PubMed: 11156601]

Wang YP, Dakubo G, Howley P, Campsall KD, Mazarolle CJ, Shiga SA, Lewis PM, McMahon AP, and Wallace VA (2002). Development of normal retinal organization depends on Sonic hedgehog signaling from ganglion cells. Nat. Neurosci 5, 831–832. [PubMed: 12195432]

Author Manuscript Author Manuscript Author Manuscript Author Manuscript

Highlights

- Six3 and Six6 are jointly required to maintain multipotent retinal progenitors
- Six3 and Six6 together suppress Wnt/β-catenin signaling
- Six3 and Six6 together maintain the expression of multiple retinogenic factors
- Wnt3a/β-catenin signaling promotes ciliary margin cells at the cost of neuroretina

Author Manuscript Author Manuscript Author Manuscript Author Manuscript

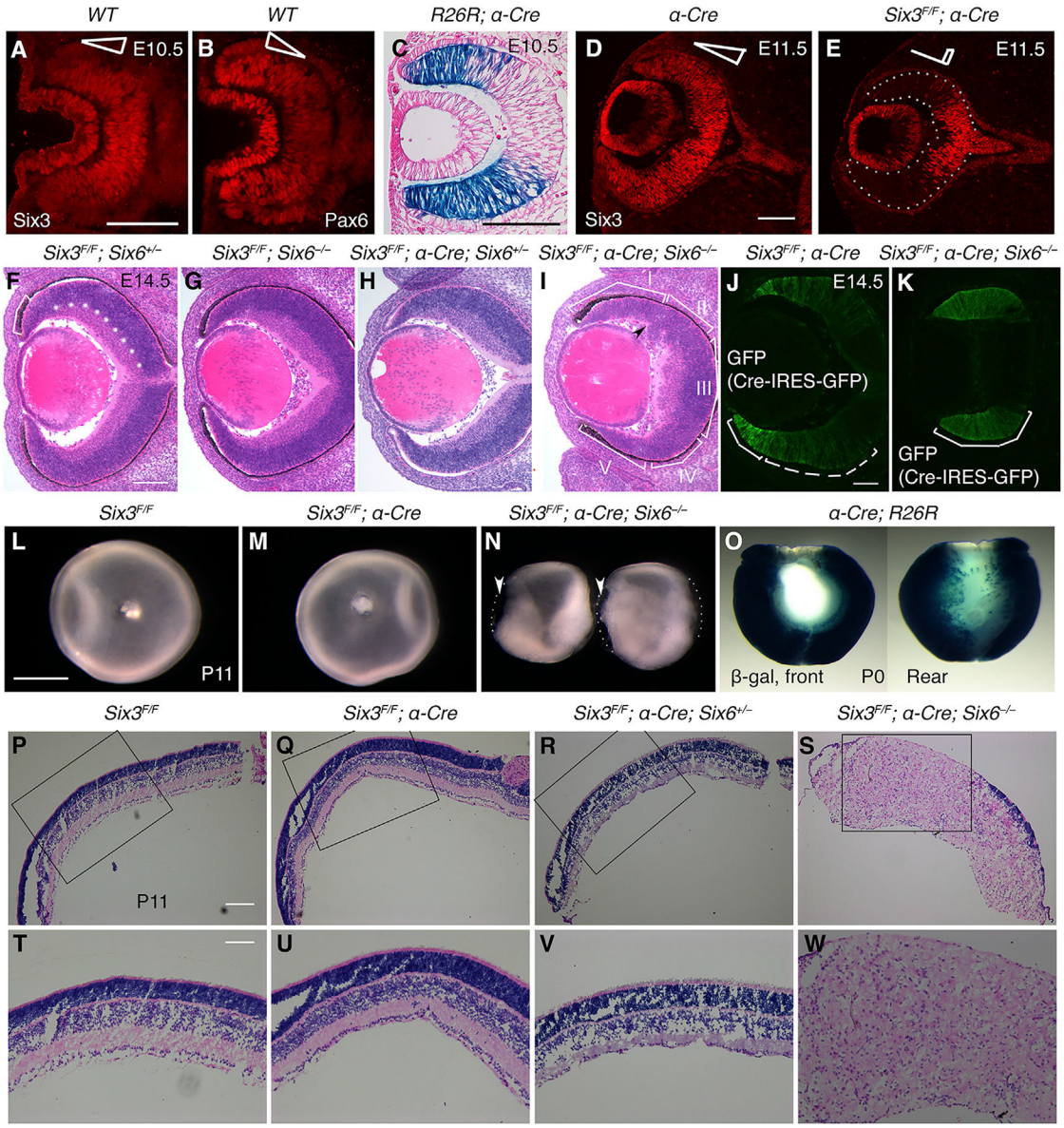

Figure 1. A Gradient of Six3 Expression in E10.5–11.5 Neuroretina and Morphological Abnormalities Caused by *Six3* and *Six6* Compound Deletion (DKO)

(A and B) Six3 expression displayed a gradient with high levels in central NR (A), whereas Pax6 expression exhibited an inverse gradient (B).

(C) R26R reporter expression for *α-Cre* was detected in peripheral NR as early as E10.5.

(D and E) Graded Six3 expression remained in E11.5 NR (D). Six3 protein deletion was detected in peripheral NR as early as E11.5 (E).

(F–I) At E14.5, newly differentiated retinal neurons and NR progenitors formed two layers in $Six3^{F/F};Six6^{+/-}$ retinas (dotted line in F), $Six3^{F/F};Six6^{-/-}$retinas (G), and $Six3^{F/F}$;*α-Cre*;$Six6^{+/-}$retinas (H). In peripheral DKO retinas, the layer of newly differentiated neurons was absent; an abrupt change in retinal thickness was found, resulting in far- and mid-peripheral regions (arrowhead in I; see also Figures 2D and 3D for efficient *Six3* deletion).

Author Manuscript Author Manuscript Author Manuscript Author Manuscript

(J and K) GFP (Cre-IRES-GFP) expression was expanded in E14.5 DKO retinas (K) compared to that in *Six3*$^{F/F}$; *α-Cre* retinas (J).

(L–N) On postnatal day 11, *Six3*$^{F/F}$ retinas (L) and *Six3*$^{F/F}$;*α-Cre* retinas (M) were translucent, but DKO retinas were opaque except for in a narrow central band (N). Severe degenerations were found at the far-peripheral regions of DKO retinas (arrowheads in N).

(O) At postnatal day 0, R26R reporter for *α-Cre* was widely expressed in the retina except for in a narrow central band.

(P–W) On sections, unlike *Six*$^{3F/F}$ retinas (P and T) and *Six*$^{3F/F}$; *α-Cre* retinas (Q and U) and *Six*$^{3F/F}$; *α-Cre;Six6*$^{+/-}$ retinas (R and V), DKO retinas lacked a laminar structure and comprised sparsely dispersed cells (S and W).

Scale bars, 100 μm (A, C, D, F, J, and T), 200 μm (P), 1 mm (L). n = 3 embryos. See also Figures S1–S7.

Author Manuscript Author Manuscript Author Manuscript Author Manuscript

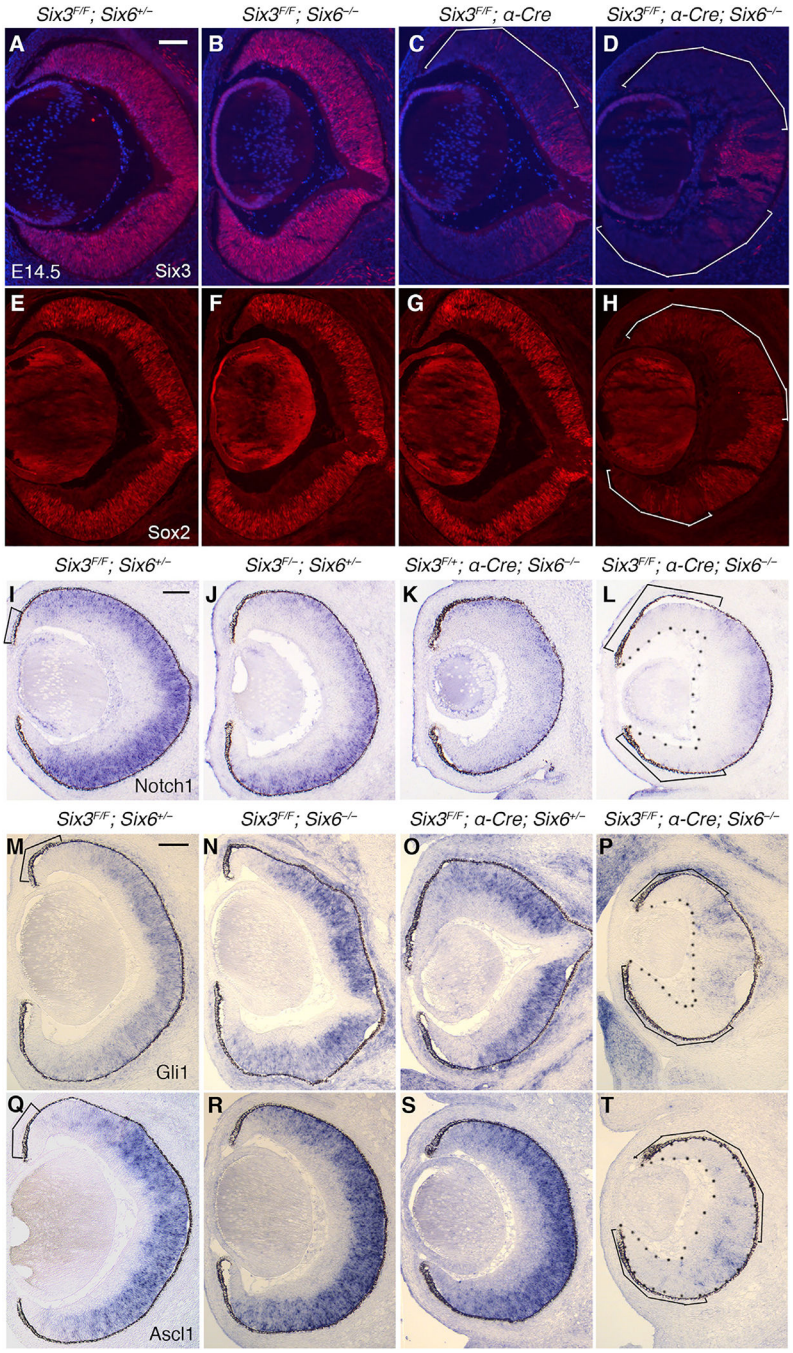

Figure 2. NR Progenitors Are Defective in E14.5 DKO Retinas

(A–D) Six3 was expressed in *Six3*$^{F/F}$;*Six6*$^{+/-}$ retinas (A) and *Six3*$^{F/F}$;*Six6*$^{-/-}$ retinas (B), but was deleted except for in a narrow central band in *Six3*$^{F/F}$;*α-Cre* retinas (C) and DKO retinas (D).

(E–H) Compared to that in *Six3*$^{F/F}$;*Six6*$^{+/-}$ retinas (E), Sox2 was unaffected in *Six3*$^{F/F}$;*Six6*$^{-/-}$ retinas (F) and *Six3*$^{F/F}$;*α-Cre* retinas (G) but was reduced in the peripheral regions of DKO retinas (H).

Author Manuscript Author Manuscript Author Manuscript Author Manuscript

(I–L) Notch1 was nearly absent in the peripheral regions of DKO retinas (L) compared to that in *Six3*$^{F/F}$;*Six6*$^{+/-}$ retinas (I), *Six3*$^{F/-}$;*Six6*$^{+/-}$ retinas (J), and *Six3*$^{F/F}$;*α-Cre*;*Six6*$^{+/-}$ retinas (K).

(M–P) Compared to that in *Six3*$^{F/F}$;*Six6*$^{+/-}$ retinas (M), Gli1 was unaffected in *Six3*$^{F/F}$;*Six6*$^{-/-}$ retinas (N) and *Six3*$^{F/F}$;*α-Cre*;*Six6*$^{+/-}$ retinas (O) but was absent or severely reduced in DKO retinas (P).

(Q–T) Compared to that in *Six3*$^{F/F}$;*Six6*$^{+/-}$ retinas (Q), Asc1 was unaffected in *Six3*$^{F/F}$;*Six6*$^{-/-}$ retinas (R) and *Six3*$^{F/F}$;*α-Cre*;*Six6*$^{+/-}$ retinas (S) but was absent or severely reduced in DKO retinas (T).

Scale bars, 100 μm (A, I, and M). n = 3 embryos. See also Figures S2 and S3.

Author Manuscript Author Manuscript Author Manuscript Author Manuscript

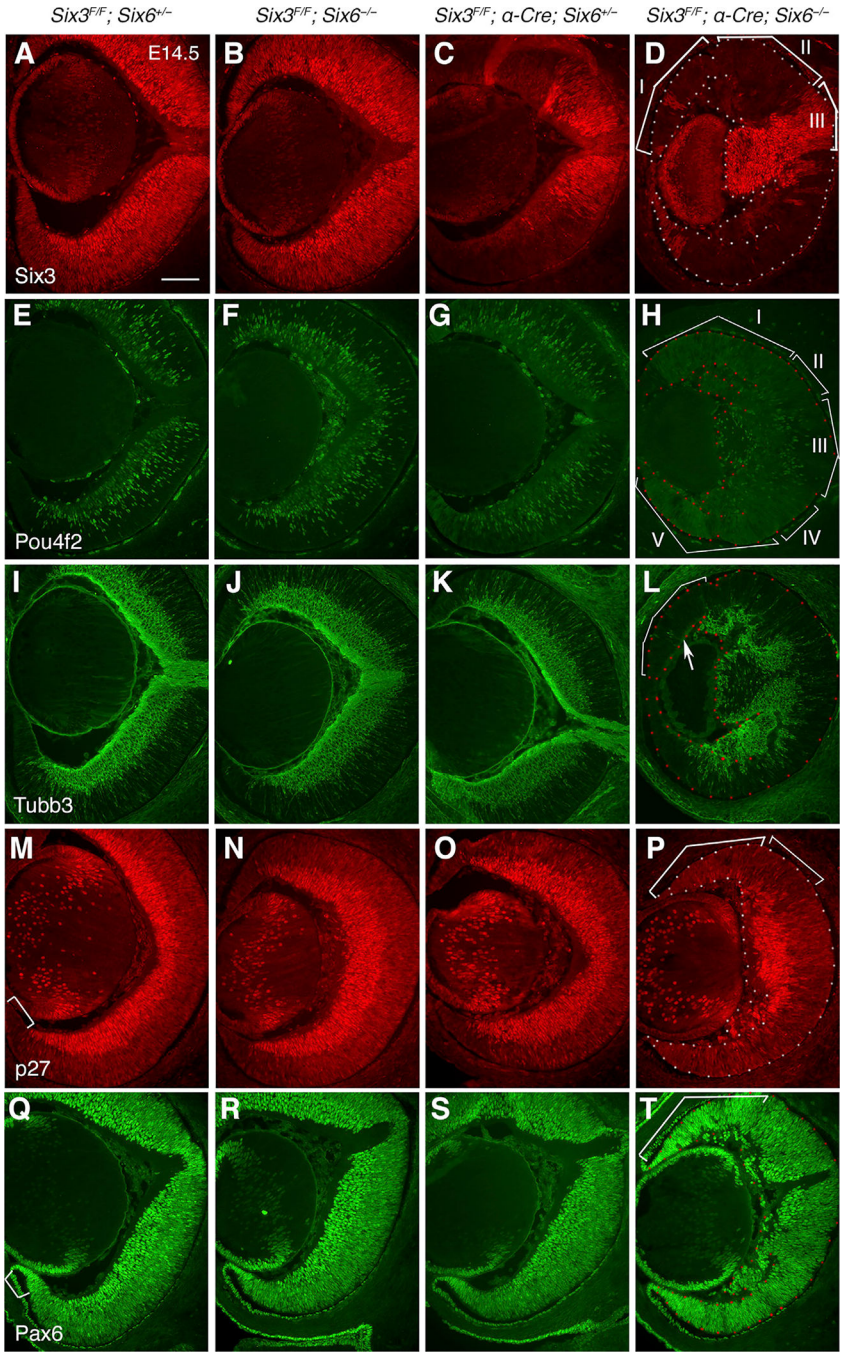

Figure 3. Early Retinal Differentiation Is Affected in E14.5 DKO Retinas

(A–D) Six3 was expressed in $Six3^{F/F};Six6^{+/-}$ retinas (A) and $Six3^{F/F};Six6^{-/-}$ retinas (B), but was efficiently deleted in $Six3^{F/F};\alpha\text{-}Cre;Six6^{+/-}$ retinas (C) and DKO retinas (D).

(E–H) Compared to that in $Six3^{F/F};Six6^{+/-}$ retinas (E), Pou4f2 was unaffected in $Six3^{F/F};Six6^{-/-}$ retinas (F) and $Six3^{F/F};\alpha\text{-}Cre;Six6^{+/-}$ (G) retinas. In DKO retinas, Pou4f2 was nearly absent in far-peripheral regions (H, areas I and V) and reduced in mid-peripheral regions (H, areas II and IV).

Author Manuscript Author Manuscript Author Manuscript Author Manuscript

(I–P) Compared to those in *Six3*$^{F/F}$;*Six6*$^{+/-}$ retinas (I and M), Tubb3 and p27 were unaffected in *Six3*$^{F/F}$; *Six6*$^{-/-}$ retinas (J and N) and *Six3*$^{F/F}$;*α-Cre*;*Six6*$^{+/-}$ retinas (K and O) but were significantly reduced in far-peripheral regions of DKO retinas (L and P).
(Q–T) Compared to that in *Six3*$^{F/F}$;*Six6*$^{+/-}$ retinas (Q), Pax6 was unaffected in *Six3*$^{F/F}$;*Six6*$^{-/-}$ retinas (R) and *Six3*$^{F/F}$;*α-Cre;Six6*$^{+/-}$ retinas (S) but was increased in far-peripheral regions of DKO retinas (T).
Scale bar, 100 μm. n = 3 embryos.

Author Manuscript Author Manuscript Author Manuscript Author Manuscript

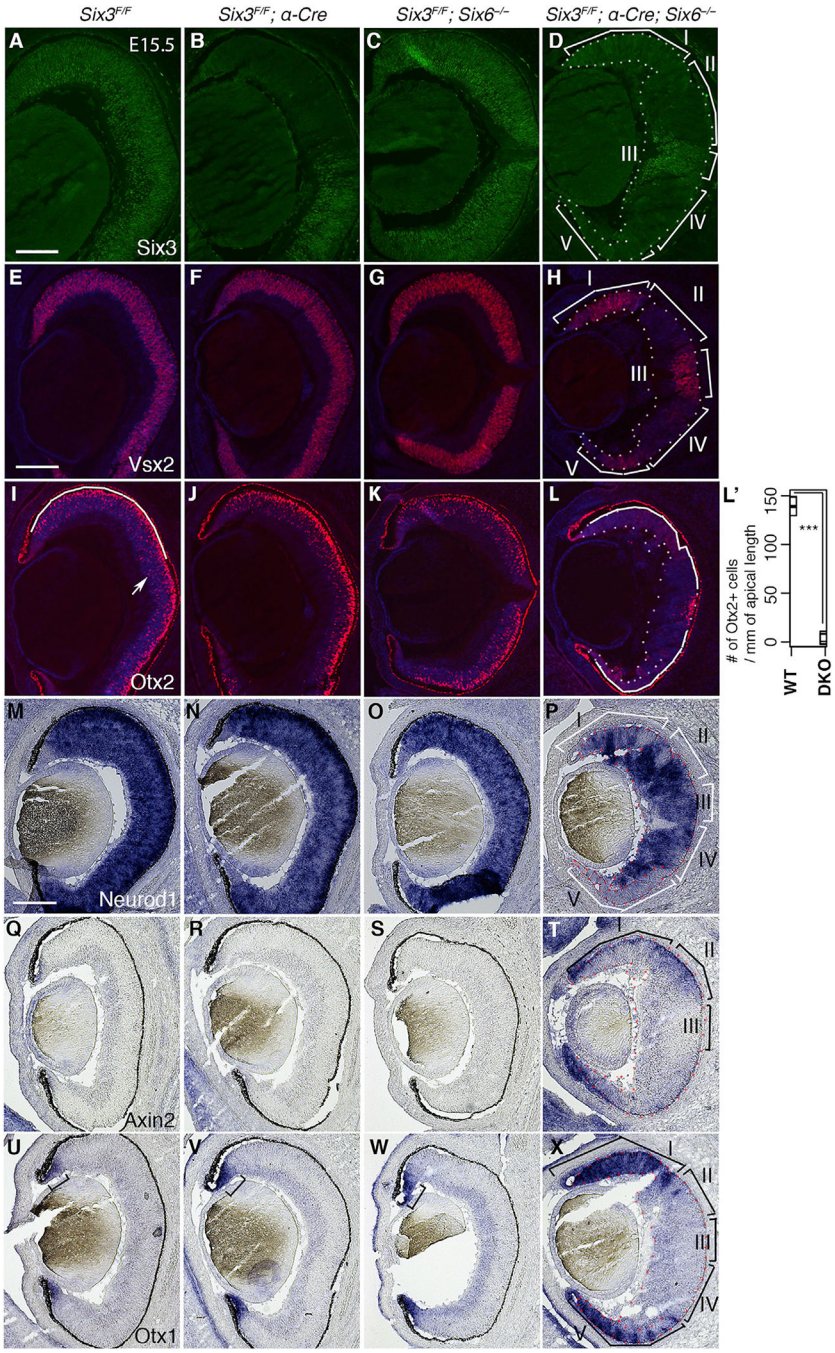

Figure 4. Loss of NR Identity Is Accompanied by Ectopic Upregulation of Wnt/β-Catenin Signaling and CM Markers in E15.5 DKO Retinas

(A–D) Six3 was expressed in *Six3*$^{F/F}$ retinas (A), but was efficiently deleted in *Six3*$^{F/F}$;*α-Cre* retinas (B) and DKO retinas (D). Six3 was unaffected in *Six6* null retinas (C).

(E–H) Compared to that in *Six3*$^{F/F}$ retinas (E), Vsx2 was unaffected in *Six3*$^{F/F}$;*α-Cre* retinas (F) and *Six3*$^{F/F}$;*Six6*$^{-/-}$ retinas (G). In DKO retinas, Vsx2 was absent in mid-peripheral regions (H, areas II and IV) but was present in far-peripheral regions (H, areas I and V). Vsx2 remained where Six3 was present (H, area III).

Author Manuscript Author Manuscript Author Manuscript Author Manuscript

(I–L) Compared to that in *Six3*$^{F/F}$ retinas (I), Otx2 was unaffected in *Six3*$^{F/F}$;*α-Cre* retinas (J) and *Six3*$^{F/F}$;*Six6*$^{-/-}$ retinas (K). In DKO retinas, Otx2 was nearly absent where Six3 was deleted (L). Quantification represented three eyes (L'; $^{***}p < 0.001$ in t test).
(M–P) Compared to that in *Six3*$^{F/F}$ retinas (M), Neurod1 was unaffected in *Six3*$^{F/F}$;*α-Cre* retinas (N) and *Six3*$^{F/F}$;*Six6*$^{-/-}$ retinas (O). In DKO retinas, Neurod1 was absent (P, area V) or severely reduced (P, areas I) in far-peripheral regions but remained in mid-peripheral regions with disrupted stratification (P, area II).
(Q–T) Compared to that in *Six3*$^{F/F}$ retinas (Q), Axin2 was unaffected in *Six3*$^{F/F}$;*α-Cre* retinas (R) and *Six3*$^{F/F}$;*Six6*$^{-/-}$ retinas (S). In DKO retinas, Axin2 was ectopically upregulated in both far- and mid-peripheral regions (T, areas I, II, IV, and V).
(U–X) Compared to that in *Six3*$^{F/F}$ retinas (U), Otx1 was unaffected in *Six3*$^{F/F}$;*α-Cre* retinas (V) and *Six3*$^{F/F}$;*Six6*$^{-/-}$ retinas (W). In DKO retinas, Otx1 expression was ectopically upregulated in far-peripheral regions (X, areas I and V).
Scale bars, 200 μm. n = 3 embryos. See also Figure S5.

Author Manuscript Author Manuscript Author Manuscript Author Manuscript

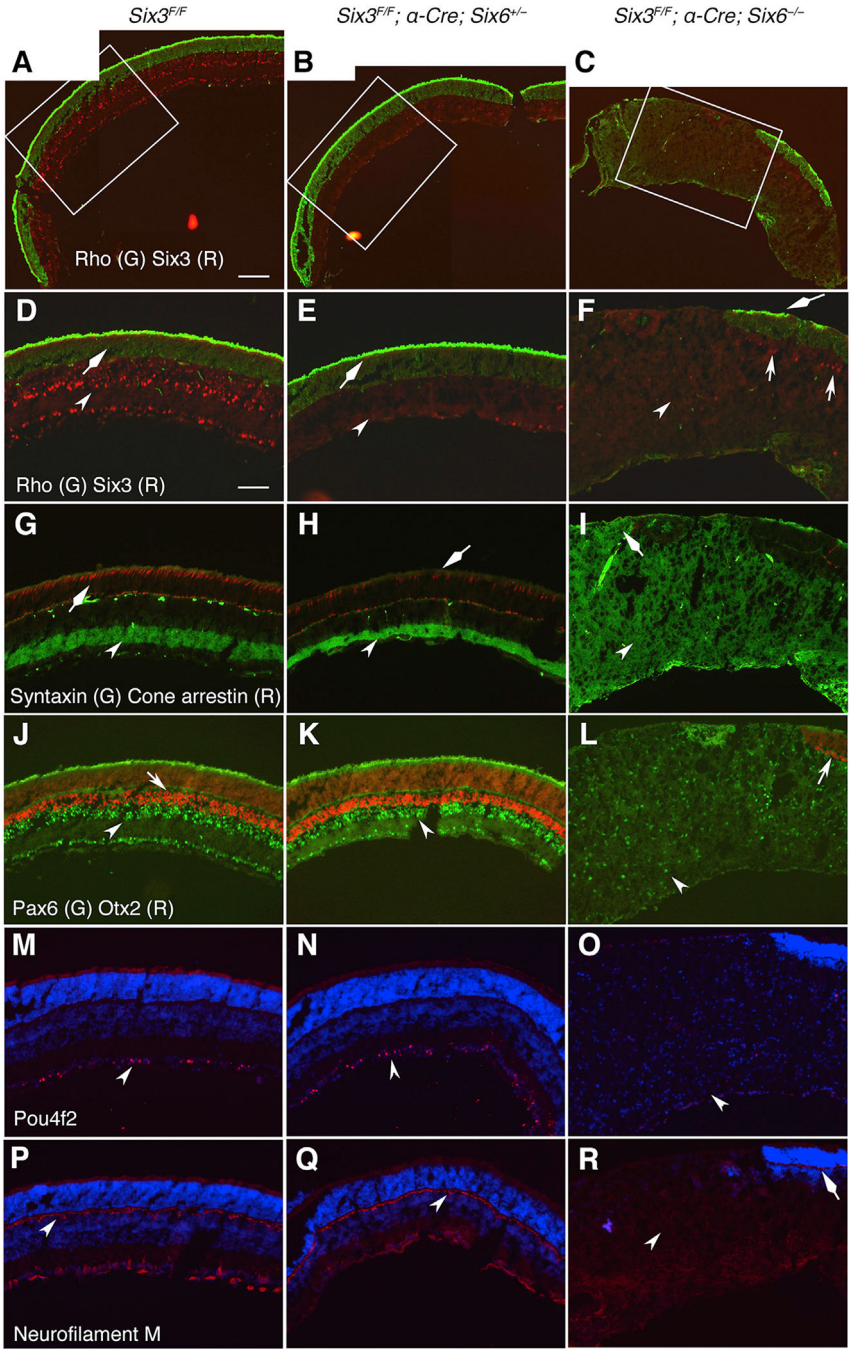

Figure 5. DKO Retinas at Postnatal Day 11 Lack a Laminar Structure and Comprise Only a Subpopulation of Amacrine Cells and Infiltrated Astrocytes

(A–F) Six3 was expressed in *Six3*$^{F/F}$ retinas (A and D), but was efficiently deleted in *Six3*$^{F/F}$; *α-Cre*;*Six6*$^{+/-}$ retinas (B and E) and DKO retinas (C and F). Rho was unaffected in *Six3*$^{F/F}$;*α-Cre;Six6*$^{+/-}$ retinas (B and E) compared to that in *Six3*$^{F/F}$ retinas (A and D). DKO retinas lacked a laminar structure and did not express Rho where Six3 was absent (F). (A) and (B) are stitched images to have broader views of the retina.

(G–L) Compared to *Six3*$^{F/F}$ retinas (G and J) and *Six3*$^{F/F}$;*α-Cre*;*Six6*$^{+/-}$ retinas (H and K), DKO retinas did not express either cone arrestin (I) or Otx2 (L) but widely expressed

Author Manuscript Author Manuscript Author Manuscript Author Manuscript

syntaxin (I) and Pax6 (L). (M–R) Compared to *Six3*$^{F/F}$ retinas (M and P) and *Six3*$^{F/F}$;*α-Cre*;*Six6*$^{+/-}$ retinas (N and Q), DKO retinas did not express either Pou4f2 (O) or neurofilament M (R).

Scale bars, 200 μm (A), 100 μm (D). n = 3 retinas.

See also Figures S6 and S7.

Author Manuscript Author Manuscript Author Manuscript Author Manuscript

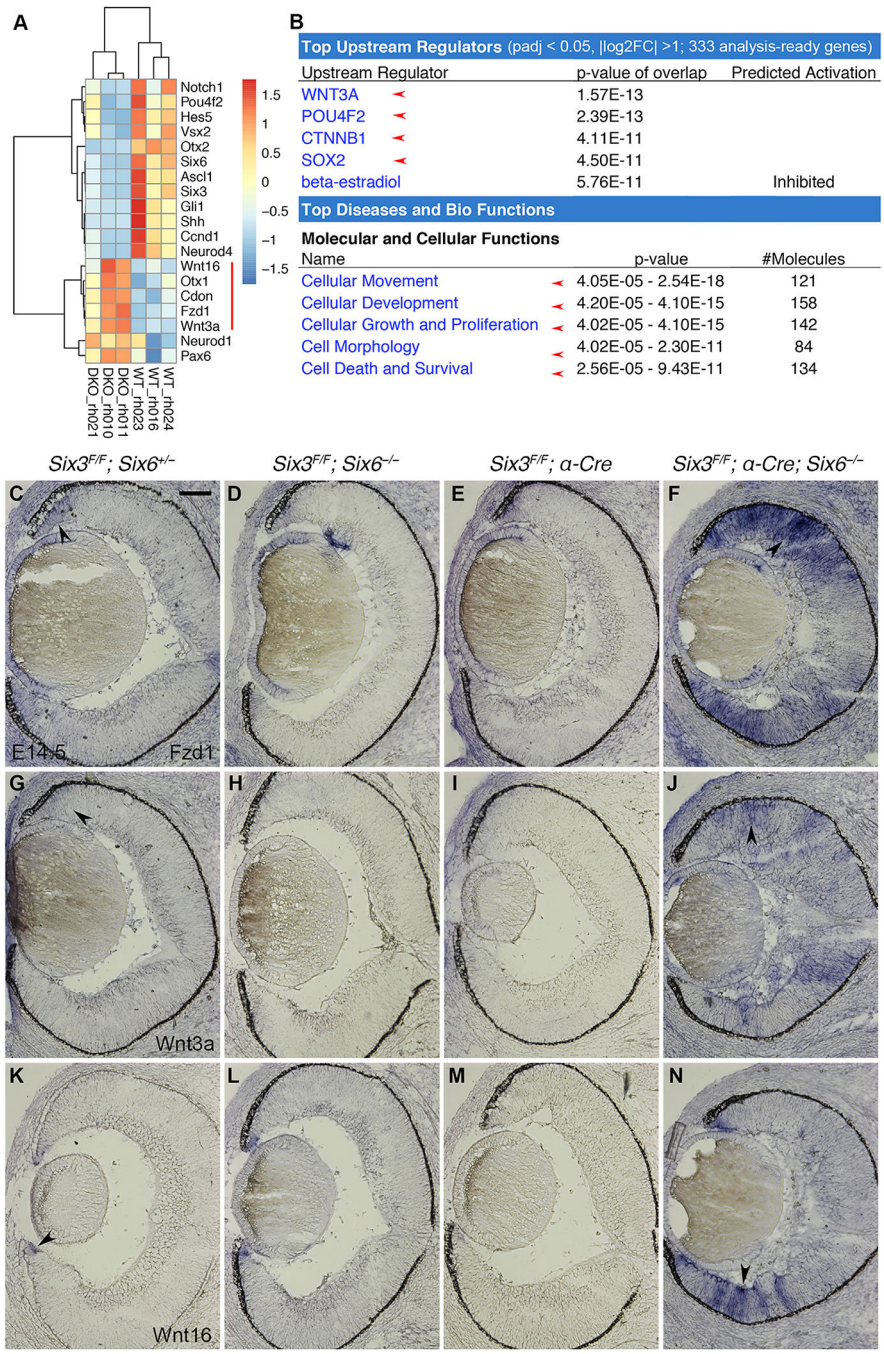

Figure 6. The Gene Set Jointly Regulated by Six3 and Six6 Highly Overlaps with the Gene Networks Regulated by WNT3A, CTNNB1, POU4F2, or SOX2

(A) RNA-seq not only confirmed most known DEGs but also identified additional DEGs, e.g., *Fzd1*, *Wnt3a*, Cdon, and *Wnt16*, in DKO retinas. Normalized counts generated using DESeq2 were used for plotting. The DEGs are in Table S2.

(B) The gene set jointly regulated by Six3 and Six6 highly overlapped with the GRNs regulated by WNT3A, CTNNB1, POU4F2, or SOX2, which were among the top five upstream regulators in IPA. The predicted functions of DEGs matched the observed phenotypes.

Author Manuscript Author Manuscript Author Manuscript Author Manuscript

(C–N) Fzd1 (C–F), Wnt3a (G–J), and Wnt16 (K–N) were upregulated in E14.5 DKO retinas (F, J, and N) compared to those in *Six3*$^{F/F}$;*Six6*$^{+/-}$ retinas (C, G, and K), *Six3*$^{F/F}$;*Six6*$^{-/-}$ retinas (D, H, and L), and *Six3*$^{F/F}$;*α-Cre* retinas (E, I, and M). Six3 deletion was shown in Figures 2A–2D.

Scale bar, 100 μm (C). n = 3 embryos

Author Manuscript Author Manuscript Author Manuscript Author Manuscript

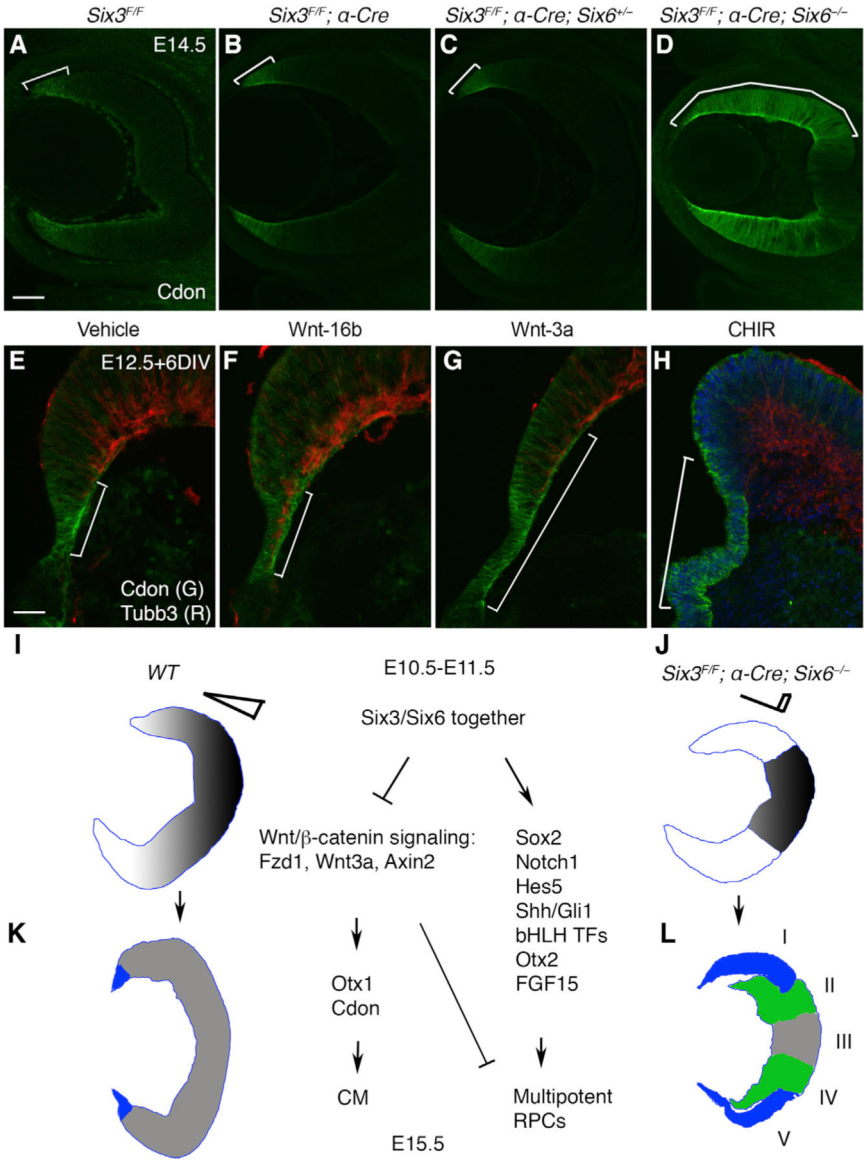

Figure 7. Stimulation of Wnt/β-Catenin Signaling by Either Wnt-3a or a GSK3β Inhibitor Promotes CM Cell Fate at the Cost of NR Identity at the Periphery of Mouse Eyecups

(A–D) CM marker Cdon was expanded in E14.5 DKO retinas (D) compared to that in *Six3*$^{F/F}$ retinas (A), *Six3*$^{F/F}$;*α-Cre* retinas (B), and *Six3*$^{F/F}$;*α-Cre*; *Six6*$^{+/-}$ retinas (C).

(E–H) Compared to vehicle controls (E), Wnt-3a (G) or GSK3β inhibitor CHIR99021 (H), but not Wnt-16b (F), expanded the size of CM (Cdon-positive Tubb3-negative) at the cost of NR identity at the periphery of mouse eyecups.

(I–L) A working model. At E10.5–11.5, both Six3 and Six6 expression displayed a gradient along peripheral-central axis (I). In most-peripheral regions, low levels of Six3 and Six6 permitted Wnt/ β-catenin signaling, leading to CM specification (blue in (K), an illustration of Otx1 expression in E15.5 control retina in Figure 4U). Moving centrally in the neuroretina, high levels of Six3 and Six6 protected multipotent NR progenitors directly or indirectly through (1) suppressing Wnt/β-catenin signaling and (2) maintaining the expression of retinogenic factors. When *Six3* was deleted in E10.5 neuroretina using *α-Cre*

Author Manuscript Author Manuscript Author Manuscript Author Manuscript

in combination with *Six6* deletion (J), the suppression of Wnt/β-catenin signaling was removed and the expression of retinogenic factors was disrupted. Retinal cells in far-peripheral regions gained CM identity at the expense of NR progenitors under the stimulation of Wnt/β-catenin signaling, whereas retinal cells in mid-peripheral regions maintained NR identity but lost multipotency (L, an illustration of Otx1 and Neurod1 expression in E15.5 DKO retinas in Figures 4P and 4X).
Scale bars, 100 μm (A), 50 μm (E). n = 3 retinas.

Author Manuscript Author Manuscript Author Manuscript Author Manuscript

KEY RESOURCES TABLE

REAGENT or RESOURCE	SOURCE	IDENTIFIER
Antibodies		
Goat polyclonal anti-Choline Acetyltransferase	Millipore	Cat#AB144P; RRID:AB_2079751
Rabbit polyclonal anti-Cone Arrestin	Millipore	Cat#AB15282; RRID:AB_11210270
Mouse monoclonal anti-GAD65	Fisher Scientific	Cat#BDB559931; RRID:AB_397380
Rabbit polyclonal anti-GABA	Sigma	Cat#A2052; RRID:AB_477652
Rabbit polyclonal anti-GFAP	Sigma	Cat#G9269; RRID:AB_477035
Mouse monoclonal anti-Glutamine Synthetase(also known as Glul)	BD Bioscience	Cat#610517; RRID:AB_2313837
Goal polyclonal anti-Glycine Transporter 1	Millipore	Cat#AB1770; RRID:AB_90893
Rat monoclonal anti-Laminin-1 A&B	Millipore	Cat#MAB1904; RRID:AB_2133631
Goal polyclonal anti-Lhx2	Santa Cruz	Cat#sc-19344; RRID:AB_2135660
Rabbit polyclonal anti-Neurofilament M	Millipore	Cat#AB1987; RRID:AB_91201
Goat polyclonal anti-Otx2	R&D Systems	Cat#AF1979; RRID:AB_2157172
Rabbit polyclonal anti-p27	Santa Cruz	Cat#sc776; RRID:AB_2276045
Rabbit polyclonal anti-Pax6	Covance	Cat# PRB-278P, RRID:AB_291612
Rabbit polyclonal anti-pH3	Upstate	Cat#06–570; RRID:AB_310177
Rabbit polyclonal anti- PRKC zeta (Prkcz)	Santa Cruz	Cat#sc-216; RRID:AB_2300359
Mouse monoclonal anti-Rhodopsin (Rho 4D2)	Abcam	Cat#ab98887; RRID:AB_10696805
Rabbit polyclonal anti-Six3	Rockland	Cat#600–401-A26; RRID:AB_11180063
Rabbit polyclonal anti-Sox2	Chemicon	Cat#AB5770
Rabbit polyclonal anti-Syntaxin	Sigma	Cat#S0664; RRID:AB_10641968
Rabbit polyclonal anti-Tyrosine Hydroxylase	Millipore	Cat#AB152; RRID:AB_390204
Mouse monoclonal anti-Tubb3 (also known as Tuj1)	BabCO	Cat#MMS435P; RRID:AB_2313773
Sheep monoclonal anti-Vsx2	Abcam	Cat#AB9016; RRID:AB_2216009
Chemicals, Peptides, and Recombinant Proteins		
Recombinant Human Wnt-3a Protein	R&D Systems	Cat# 5036-WN-010
Recombinant Human Wnt-16b Protein	R&D Systems	Cat# 7790-WN
CHIR99021	TOCRIS	Cat#4423
Deposited Data		
RNA-seq of mouse embryonic retinas at E13.5	This paper	GEO: GSE115258
Experimental Models: Organisms/Strains		
Mouse: $Six3^{F/F}$	Guillermo Oliver: Liu et al., 2006	N/A
Mouse: $Six6^{-//-}$	Michael Rosenfeld: Li et al., 2002	N/A

Author Manuscript Author Manuscript Author Manuscript Author Manuscript

REAGENT or RESOURCE	SOURCE	IDENTIFIER
Mouse: α-Cre	Peter Gruss: Marquardt et al., 2001	N/A
Mouse: CAGGCre-ERM^{TM}	The Jackson Laboratory	JAX: 004682
Recombinant DNA		
Fzd1 (NM_021457) Mouse Tagged ORF Clone	Origene	Cat#MR209705
Wnt3a (NM_009522) Mouse Tagged ORF Clone	Origene	Cat#MR227165
Wnt16 (NM_053116) Mouse Tagged ORF Clone	Origene	Cat#MR222522
Hes1 (NM_008235) Mouse Tagged ORF Clone	Origene	Cat#MR203818
Ascl1 template plasmid	Marquardt et al., 2001	N/A
Atoh7 template plasmid	Brown et al., 1998	N/A
Axin2 template plasmid	Jho et al., 2002	N/A
Fgf15 template plasmid	Burns et al., 2008	N/A
Fzd5 template plasmid	Burns et al., 2008	N/A
Foxn4 template plasmid	Li et al., 2004	N/A
Gli1 template plasmid	Cwinn et al., 2011	N/A
Hes5 template plasmid	Taranova et al., 2006	N/A
Neurog2 template plasmid	Marquardt et al., 2001	N/A
Neurod1 template plasmid	Li et al., 2004	N/A
Neurod4 template plasmid	Inoue et al., 2002	N/A
Notch1 template	Taranova et al., 2006	N/A
Otx1 template plasmid	Cwinn et al., 2011	N/A
p57 template plasmid	Li et al., 2002	N/A
Shh template	Cwinn et al., 2011	N/A
Six6 template plasmid	Li et al., 2002	N/A
Software and Algorithms		
Trim Galore(v. 0.3.7)	Babraham Bioinformatics	https://www.bioinformatics.babraham.ac.uk/projects/trim_galore/
Tophat (v. 2.0.13)	Trapnell et al., 2009	https://ccb.jhu.edu/software/tophat/index.shtml
HTseq (v.0.6.1)	Anders et al., 2015	https://htseq.readthedocs.io/en/release_0.10.0/
Cufflinks (v. 2.2.1)	Trapnell et al., 2010	http://cole-trapnell-lab.github.io/cufflinks/
mm10, refseq gene annotation	UCSC genome browser	https://genome.ucsc.edu/
Deseq2	Love et al., 2014	https://bioconductor.org/packages/release/bioc/html/DESeq2.html
Ingenuity Pathway Analysis (IPA)	QIAGEN bioinformatics	https://www.qiagenbioinformatics.com/